People's Democratic Republic of Algeria
Ministry of Higher Education and Scientific Research
University A.MIRA-BEJAIA

Faculty of Technology
Department of Electrical Engineering

Thesis submitted in partial fulfillment of the requirements for the degree of Masters of Science in Electrical Engineering
Option: Electrical Networks

Thème

Transient Stability Analysis of a Grid Connected Wind Farm

Prepared by:

CHINHAMO Simbarashe

Supervised by:

Professor MEDJDOUB Abdellah

Academic Year: 2023/2024

ACKNOWLEDGEMENTS

I am deeply grateful to Almighty God through Jesus Christ for His inspiration, guidance, protection, and provision throughout the completion of this Master's program. My heartfelt thanks go to my supervisor, Professor Abdellah Medjdoub, for his unwavering support and assistance, which were crucial in ensuring the successful completion of this thesis. I also extend my sincere appreciation to all the faculty and staff of the Department for their encouragement and moral support. I extend my deepest gratitude to each and every one of you.

DEDICATIONS

I dedicate this thesis, and all my endeavours, to my family. I have been consistently surrounded by the unwavering support of my brother, Albert and his wife Revai. I owe my achievements to the love and encouragement of my parents. Despite the distance, their moral and financial support has been invaluable. I say a very big thank you.

Table of Contents

CHAPTER III: TRANSIENT STABILITY ANALYSIS CONCEPT AND THEORY

CHAPTER IV: SIMULATION AND RESULTS

List of Figures

List of Tables

List of symbols and abbreviations

IEEE : Institute of Electrical and Electronics Engineers
SCIG : Squirrel Cage Induction Generator
WRIG : Wound Rotor Induction Generator
DFIG : Doubly Fed Induction Generator
WRSG : Wound Rotor Synchronous Generator
PMSG :Permanent Magnet Synchronous Generator
IEA: International Energy Agency
WWEA: World Wind Energy Association
HAWT: Horizontal Axis Wind Turbines
VAWT: Vertical Axis Wind Turbines
WTG : Wind Turbine Generators
FACTS: Flexible Alternating Current Transmission Systems
STATCOM: Static Synchronous Compensator
LSS: Low Speed Shaft
HSS: High Speed Shaft
PWM: Pulse Width Modulation
GSC: Grid Side Converter
CCT: Critical Clearance Time

CHAPTER I: GENERAL INTRODUCTION

Chapter I: General Introduction

I.1. Overview of Renewable Energy

In recent years, the global energy landscape has witnessed a substantial shift towards sustainable and renewable sources. This transition is primarily driven by the growing concerns over climate change and the environmental impact of traditional fossil fuel-based energy generation [1].

Governments, industries, and communities worldwide are increasingly recognizing the need to reduce carbon emissions and embrace cleaner energy alternatives. According to [2], the adoption of renewable energy technologies has experienced remarkable growth, with an increasing number of countries investing in and transitioning to sustainable energy sources. The International Energy Agency (IEA) reports a significant rise in the global share of renewable energy in the overall energy mix, highlighting the pivotal role these sources play in mitigating climate change and fostering energy security.

Among various renewable energy sources, wind power has emerged as a key player in the quest for sustainable energy solutions. Harnessing the kinetic energy of wind, wind power has demonstrated its potential to generate substantial amounts of electricity with relatively low environmental impact. As a clean and abundant resource, wind power contributes significantly to diversify the energy mix and reducing dependence on finite fossil fuel resources [3].

I.2. Growth of Wind Power Farms

A wind farm is a group of wind turbines located together to capture wind energy and turn it into electricity. These turbines are strategically positioned to capture the kinetic energy of the wind and convert it into mechanical energy, which is then transformed into electrical energy through generators [4].

The global expansion of wind power farms has seen a substantial increase in both capacity and installation rates, indicative of a growing commitment to sustainable energy sources. As reported by the World Wind Energy Association (WWEA), the total installed capacity of wind power has consistently risen, emphasizing the global momentum towards renewable energy [5].

Tómasson E. [6] suggested that this increase is due to ongoing improvements in wind turbine technology, improved project economics, and the implementation of supportive government policies promoting sustainable energy development. The increase in wind power installation brings both challenges and opportunities in integrating this variable

energy source into existing power grids.

Efforts are underway to address these challenges through innovative grid management strategies and energy storage solutions. Simultaneously, the integration of wind power presents opportunities for research and development, paving the way for advancements in grid technology and resilient energy systems. Figure I.1 is a clear evolution of the use of wind energy from 2015 and the prediction to 2030 [7].

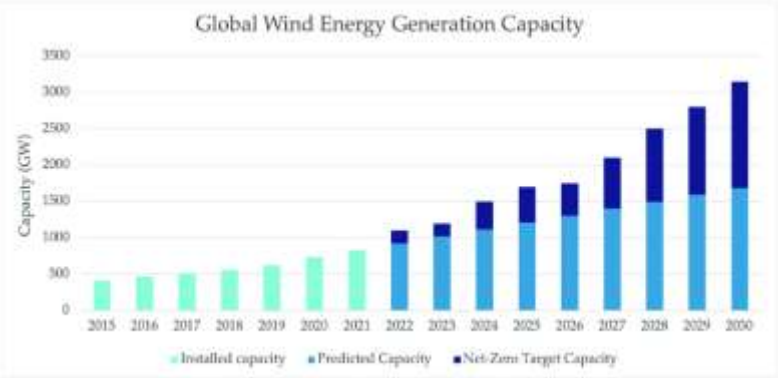

Fig I.1 Evolution of wind energy

I.3. Problem Statement

I.3.1. Need for Transient Stability Analysis

Power system stability is a critical aspect of ensuring the secure and reliable operation of electrical grids. Stability refers to the ability of a power system to maintain its equilibrium under various operating conditions, disturbances, and changes. Transient stability, specifically, focuses on the system's response to sudden and large disturbances, such as faults or disconnections. Understanding and analyzing transient stability is essential for preventing cascading failures and blackouts in power systems [7].

I.3.2. Challenges in Transient Stability of Wind Power Grids

The integration of wind power into electrical grids introduces unique challenges to transient stability. Wind power's inherent variability and uncertainty pose challenges for traditional stability assessment methods, necessitating the development of new tools and techniques for accurate analysis. Factors such as the intermittent nature of wind, varying wind speeds, and the impact of power electronics in wind turbines contribute to the complexity of transient stability issues in wind power grids [8].

I.3.3. Importance of the Study

The transient stability analysis of wind power grid-connected farms is vital for ensuring the overall reliability and security of power systems. A thorough understanding of transient stability enables the identification of potential issues and the development of

effective control strategies to prevent system failures. This is crucial for maintaining a continuous and stable supply of electricity, especially with the increasing integration of renewable energy sources like wind power into the grid.

The study of transient stability in wind power grids directly addresses the challenges associated with the integration of wind energy into existing power systems. By identifying and understanding the transient stability issues specific to wind power, this research contributes to the development of solutions and strategies for enhancing the seamless integration of wind power into the broader energy infrastructure [6,9].

I.4. Objectives of the Study

1. Conducting Transient Stability Analysis of a Wind Power Grid connected system.
2.Present a Mathematical Model for Wind Grid Connection
3. Simulation and Results

I.5. Outline of Thesis

This thesis contains 4 chapters. It is organized as follows:

Chapter 1 contains the introduction, problem statement, objective of the thesis.

Chapter 2 presents wind energy generation, the structure of a wind turbine and how it works followed by principles of wind power conversion and types of generators used in wind power systems.

Chapter 3 presents the study of transient stability analysis concept and theory which looks into challenges and issues associated with transient stability in wind grids as well as transient stability assessment methods. It also gives detailed models of DFIG, IEEE 9_Bus system and controls of the induction generator.

Chapter 4 presents the results of simulation ran using MATLAB/Simulink. In this last chapters we study the IEEE 9-Bus system and integrate it with a wind farm to study the transients behaviour of the integrated power grid. We present results of the wind farm and then integrated system of IEEE 9-Bus system. We end our work with a general conclusion.

CHAPTER II: WIND ENERGY GENERATION

II.1. Introduction to Wind Power Generation

II.1.1. History and Evolution of Wind Power

The utilization of wind energy dates back thousands of years, with historical evidence of wind-powered machines being used for various purposes. One of the earliest known applications of wind power is the sailing of ships, which dates back to ancient civilizations such as the Egyptians and Phoenicians. It wasn't until the late 19th and early 20th centuries that wind energy started being used for generating electricity on a larger scale [10].

The first electricity-generating wind turbine was constructed by Charles F. Brush in 1888 in Cleveland, Ohio, USA. This turbine, known as the Brush Windmill, featured a 12 kW dynamo connected to a 17-meter diameter rotor and was used to power his mansion. Shortly after, in Denmark, Poul la Cour developed the first wind turbine specifically designed for electricity generation in 1891. La Cour's turbine featured a horizontal-axis design and was used to charge batteries for rural electrification purposes [11].

Later on, the mid-20th century saw advancements in wind turbine technology, particularly with the development of aerodynamic designs and blade shapes. In the 1940s, the Smith-Putnam wind turbine was installed in Vermont, USA, marking the first grid-connected wind turbine to provide electricity to a local utility grid. However, it wasn't until the 1970s and 1980s that wind energy experienced significant growth and commercialization, driven by the oil crises and growing environmental concerns [12].

II.1.2. Basics of Wind Turbine Technology

II.1.2.1. Types of Wind Turbines

Wind turbines are classified into two main types based on the orientation of their axis; horizontal axis wind turbines (HAWTs) and vertical axis wind turbines (VAWTs). Each type has its unique design characteristics:

a) Horizontal Axis Wind Turbines (HAWTs)

Horizontal Axis Wind Turbines (HAWTs) are the predominant type of wind turbine used for large-scale electricity generation worldwide. In HAWTs, the rotor shaft is positioned horizontally, perpendicular to the ground, with the blades attached to a central hub as shown in Figure II.1 [13]. These turbines are designed to capture wind energy efficiently by facing into the wind, allowing the blades to rotate around a horizontal axis. Typically, HAWTs feature three blades, although variations with two or more blades exist. The power generation components, including the generator and gearbox, are usually housed at the top of the tower. HAWTs are known for their high efficiency and reliability, making

them the preferred choice for commercial wind farms due to their ability to generate significant amounts of electricity from wind energy [14].

Fig II.1 Horizontal Axis Wind Turbines[13]

a) Vertical Axis Wind Turbines (VAWTs)

Vertical Axis Wind Turbines (VAWTs) are an alternative type of wind turbine design characterized by their vertical orientation of the rotor shaft. Unlike Horizontal Axis Wind Turbines (HAWTs), VAWTs have blades that rotate around a vertical axis, perpendicular to the ground as shown in Figure II.2. This unique configuration allows VAWTs to capture wind energy from any direction making them suitable for turbulent wind conditions and urban environments [15].

Fig II.2 Vertical Axis Wind Turbines[14]

II.1.2.2. Components of a Wind Turbine

a) Rotor Blades and Rotor Hub: The rotor blades are aerodynamic structures attached to the rotor hub. They capture wind energy and convert it into rotational mechanical energy. The rotor hub is the central component to which the rotor blades are attached. It transfers the rotational energy from the blades to the main shaft [14].

b) Nacelle: The nacelle is a protective housing that encloses the main components of the wind turbine, including the gearbox, generator, and control systems. It is mounted at the top of the tower and rotates to align with the wind direction for optimal energy capture[5].

c) Generator: The generator is the component responsible for converting the mechanical energy from the turbine's rotation into electrical energy. It typically consists of a rotor and a stator, with the rotor connected to the main shaft and the stator connected to the turbine's tower[14].

d) Tower: The tower is the tall structure that supports the wind turbine above the ground. It provides elevation for the turbine rotor to capture higher wind speeds and may be constructed from steel, concrete, or composite materials[5].

e) Electronic components: The electrical components within a wind turbine consist of the generator, the grid feedback system for electricity, and an array of sensors. These sensors, which gauge factors such as temperature, wind direction, and wind speed, are strategically positioned within and around the nacelle. Their presence facilitates turbine control and monitoring, ensuring optimal performance and safety measures are maintained throughout operation[5].

Figure II.3 shows all the components of a wind turbine.

Fig II.3 Components of a Wind Turbine

II.2. Principles of Wind Power Conversion

II.2.1. Conversion of Wind Energy to Mechanical Energy

Wind energy is converted into mechanical energy through the operation of a wind turbine. When wind blows over the rotor blades of a turbine, it exerts a force on them, causing them to rotate. This rotation is transferred to a shaft connected to the rotor hub. As the rotor spins, it drives the main shaft, which in turn drives the gearbox. The gearbox increases the rotational speed of the shaft to match the optimal speed for the generator. This mechanical energy is then used to turn the generator's rotor, which ultimately generates electricity. The entire process involves the conversion of kinetic energy from the wind into mechanical energy, which is then further transformed into electrical energy [16,17].

II.2.2. Aerodynamic Principles of Wind Energy Conversion

Wind energy conversion relies on fundamental aerodynamic principles to efficiently harness the kinetic energy of moving air and convert it into usable mechanical or electrical energy. This process involves the interaction between the rotor blades of a wind turbine and the incoming wind flow. As the wind strikes the blades, it exerts a force, causing them to rotate about their longitudinal axis. This rotational motion is crucial for extracting energy from the wind and driving the turbine's power generation system [14,18].

Wind turbine first catches wind's kinetic energy which helps to drive generator to produce electricity. The kinetic energy in air with mass m moving with velocity v is given by [19, 20]:

$$\mathrm{KE} = \frac{1}{2}\mathrm{m}v^2 \qquad (2.1)$$

The power in wind is the kinetic energy per unit time and is expressed as below:

$$P_w = \frac{1}{2}\dot{\mathrm{m}}v^2 \qquad (2.2)$$

Where:

$$\dot{m} = \frac{dm}{dt} = \textit{mass flow rate} \qquad (2.3)$$

The mass flow rate $\frac{dm}{dt}$ is:

$$\frac{dm}{dt} = \rho \mathrm{A} v \qquad (2.4)$$

where ρ and A are defined as air density and the rotor effective area, respectively.

Finally, the wind power equation is;

$$P_w = \frac{1}{2}\rho A v^3 \qquad (2.5)$$

The power extracted by the turbine blades from the wind is determined by the variance between the wind powers upstream and downstream, and can be expressed as follows:

$$P_{tur} = \frac{1}{2} mass\ flow\ rate\ (v^2 - vo^2) \qquad (2.6)$$

where v is the actual wind speed or upstream wind velocity at the entrance of the rotor blades and vo is the downstream wind velocity at the exit of rotor. The mass flow rate of the air through rotating blades is then expressed as:

$$mass\ flow\ rate = \rho A \frac{v+vo}{2} \qquad (2.7)$$

The turbine power is therefore:

$$P_{tur} = \frac{1}{2}\rho A \frac{v+vo}{2}(v^2 - vo^2) \qquad (2.8)$$

Equation (2.8) is modified to be:

$$P_{tur} = \frac{1}{2}\rho A v^3 \frac{\left(1+\frac{vo}{v}\right)\left[1-\left(\frac{vo}{v}\right)^2\right]}{2} \qquad (2.9)$$

Where;

$$C_p = \frac{\left(1+\frac{vo}{v}\right)\left[1-\left(\frac{vo}{v}\right)^2\right]}{2}$$

and is the power coefficient of the rotor.

Finally the turbine power P_{tur} from equation (2.9) is rewritten as:

$$P_{tur} = \frac{1}{2}\rho A v^3 C_p \qquad (2.10)$$

The power coefficient, C_p, is thus a dimensionless parameter and is the ratio of turbine power P_{tur} to that of wind power P_w;

$$C_p = \frac{P_{tur}}{P_w} \qquad (2.11)$$

The upper limit of the coefficient of power extraction, denoted as C_p, is dictated by the Betz limit, which sets it at 0.59. This principle specifies that a turbine cannot extract more than 59.3% of the wind power available. In practical applications, the coefficient of power extraction C_p typically ranges from 25% to 40% for wind turbines. Its value is influenced by the blade pitch angle, β_{pitch} and the tip speed ratio λ_{blade}. λ_{blade} is defined as the ratio of upstream wind speed v and downstream wind speed vo [21].

$$\lambda_{blade} = \frac{v}{vo} = \frac{\omega_{tur} \times r}{v} \qquad (2.12)$$

The relationship between C_p and tip speed ratio λ_{blade} is then established by using the blade theory of turbine and is given by;

$$C_p = \frac{1}{2}(\lambda_{blade} - 0.022\beta^2 - 5.6)e^{-0.1} \qquad (2.13)$$

and is represented graphically as shown in Figure II.4 below.

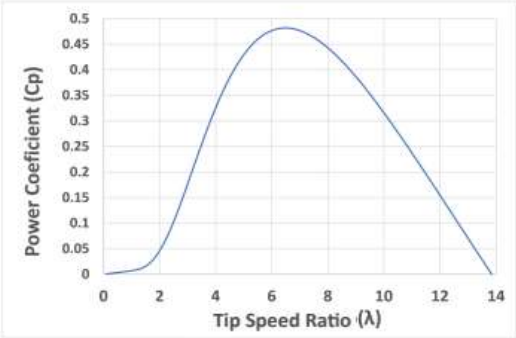

Fig II.4 Power Coefficient vs Tip Speed Ration

The maximum power is extracted when the wind turbine operates at the maximum power coefficient $C_p$max. For a typical wind turbine with a power coefficient characteristic like the one shown above, the extracted power versus the tip speed ratio is illustrated in Figure II.5. It can be seen that the aerodynamic efficiency of a wind turbine is maximal for a specific value of tip speed ratio. Therefore, by keeping the tip speed ratio at its optimum value (λ_{opt}) through the rotor speed, the maximum power at available wind speed can be extracted. Consequently, if the wind speed changes, the rotor speed must be adjusted to follow the said variation [22].

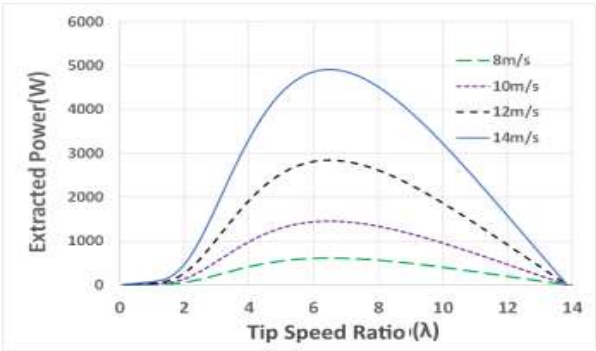

Fig II.5 Extracted Power vs Tip Speed Ratio

II.3. Types of Generators Used in Wind Power

The efficient conversion of wind energy into electrical power lies at the heart of wind power systems, with generators serving as the essential components responsible for this

conversion process. Different types of generators are utilized in wind power systems, each offering unique features, advantages, and limitations. Understanding these generator technologies is crucial for optimizing the performance and reliability of wind turbines in diverse environmental conditions. Below are types of generators used in wind power systems[23-26];

II.3.1 Asynchronous generators

Asynchronous generators, widely utilized within wind turbines, represent the most prevalent type due to their cost-effectiveness and relative simplicity compared to synchronous generators. However, a fundamental challenge arises with these generators, they necessitate the absorption of reactive power to produce a magnetic field, resulting in a flow of reactive power opposing the active power. This phenomenon poses a potential risk, particularly when the system encounters insufficient power to meet the loads, potentially leading to system collapse and consequential issues. Nevertheless, this challenge can be solved by sourcing reactive power from the grid, thereby reducing potential instability concerns. Below are the types of asynchronous generators:

II.3.1.1 Squirrel-Cage Induction Generator (SCIG)

Squirrel-Cage Induction Generators (SCIGs) are commonly used in wind turbine systems operating at fixed speeds. These generators are specifically designed to attain maximum efficiency at particular wind speeds. In typical SCIG configurations, the generator's rotor consists of a squirrel-cage winding, which allows for the generation of electrical power when the rotor is rotated by the mechanical force of the wind. SCIGs are often used in wind turbines with fixed-speed operation, where the generator's rotational speed remains constant. However, to adapt to varying wind conditions, some SCIG designs may feature two windings. This dual-winding configuration enables the generator to achieve optimal efficiency at two different wind velocities. By incorporating multiple windings, SCIGs can effectively respond to fluctuations in wind speed, thereby enhancing the overall performance and efficiency of wind turbine systems [24].

Squirrel Cage Induction Generators (SCIG) offer several advantages: their robust design with a simple rotor minimizes maintenance needs and enhances reliability. Additionally, SCIGs boast high efficiency at full load, making them economical choices for power generation. However, a key drawback is the high inrush current drawn during start-up, which can put stress on the electrical grid. Below in Figure II.6 is a typical example of a SCIG.

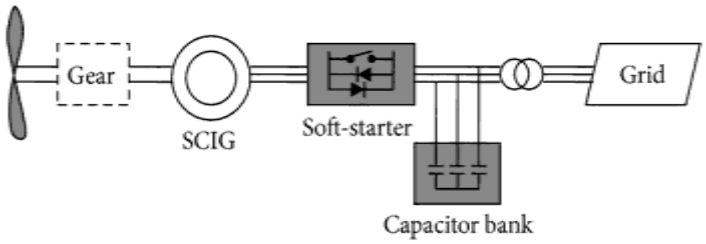

Fig II.6 Squirrel-Cage Induction Generator

II.3.1.2. Wound Rotor Induction Generators (WRIGs)

The Wound Rotor Induction Generator (WRIG) is a type of asynchronous electrical generator utilized in various applications, including wind turbine systems. Unlike conventional squirrel-cage induction generators, WRIGs feature rotor windings connected to slip rings and external resistors, enabling enhanced control over output characteristics and operating conditions. Through electromagnetic induction, the rotation of the rotor induced by external mechanical forces such as wind generates alternating current (AC) in the stator windings. This configuration allows for adjustable speed control and power output regulation, optimizing the generator's performance for different operational requirements. Despite their advantages, WRIGs also pose challenges such as increased complexity and maintenance requirements due to the presence of additional components like slip rings and brushes. Nonetheless, Wound Rotor Induction Generators remain a valuable asset in wind energy applications, offering improved efficiency and performance compared to conventional alternatives. Figure II.7 shows a typical example of a WRIG [23].

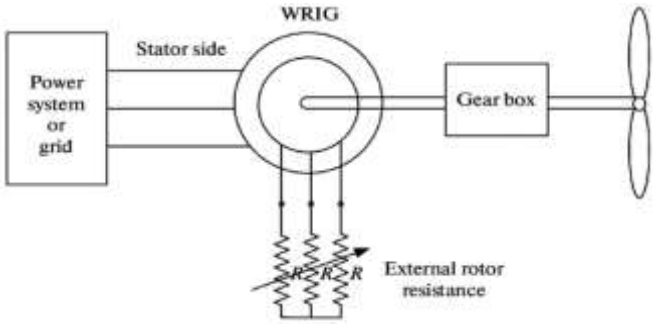

Fig II.7 Wound Rotor Induction Generators

II.3.1.3. Doubly Fed Induction Generator (DFIG)

Doubly Fed Induction Generators (DFIGs) represent a specialized type of electric generator that has gained significant traction in renewable energy applications, notably in wind turbines. Unlike traditional generators operating at fixed speeds, DFIGs feature a wound rotor configuration enabling variable-frequency AC power input. This

characteristic offers DFIGs with a crucial advantage; the ability to efficiently capture power across a range of wind speeds, thereby optimizing wind energy extraction. Furthermore, DFIGs offer the unique capability to regulate both active and reactive power, thereby enhancing power grid stability and facilitating power factor correction. Nonetheless, it's important to acknowledge a potential drawback associated with DFIGs, which pertains to their reliance on power electronics converters. While these converters enable enhanced control, they also introduce added system complexity and cost compared to simpler generator designs. Despite this challenge, the overall benefits of DFIG technology make it a compelling choice for renewable energy generation. Typical example of a doubly fed induction generator is shown in Figure II.8 [26].

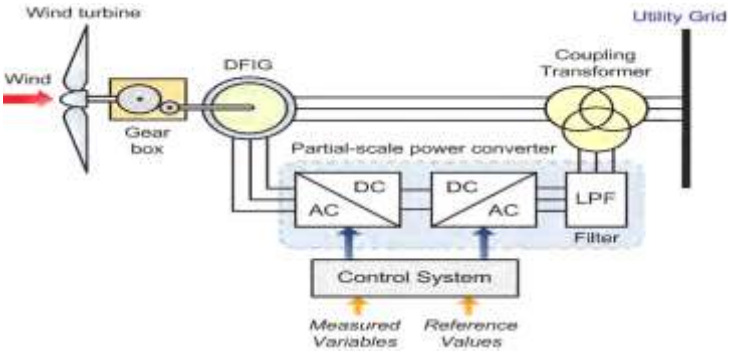

Fig II.8 Doubly Fed Induction Generator

II.3.2. Synchronous Generators

Synchronous generators, also called alternators, are pivotal in the power generation field, playing a major role in global electricity supply. Their key strength lies in maintaining a consistent frequency output, vital for grid stability and sensitive equipment operation. This frequency precision is achieved through synchronous operation, where the rotor speed is synchronized with the grid frequency. Moreover, synchronous generators can regulate reactive power, aiding in voltage control and efficient power transmission.

II.3.2.1. Permanent magnet synchronous generators (PMSG)

A Permanent Magnet Synchronous Generator (PMSG) utilizes permanent magnets to generate a magnetic field within the rotor. In a PMSG, the stator carries three separate armature windings, each displaced by 120° electrically and physically. These windings produce three-phase electromotive forces (EMFs) when the rotor, housing the permanent magnets, rotates. As the rotor spins, the magnetic field of the permanent magnets cuts across the three-phase windings, inducing EMFs in the stator windings. The permanent magnets can be fixed inside, inserted into, or mounted onto the rotor surface, depending on the generator's design. This configuration allows for efficient generation of electricity with minimal losses, making PMSGs well-suited for various

applications, including wind turbines, where they offer high efficiency, low maintenance requirements, and reliable performance. Figure II.9 shows an exemple of a PMSG [24].

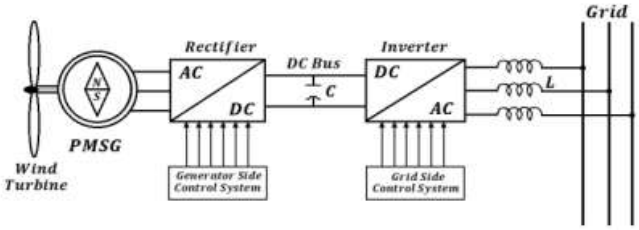

Fig II.9 Permanent magnet synchronous generators

II.3.2.2. Wound Rotor Synchronous Generator

The wound rotor synchronous generator stands as a cornerstone in the realm of electrical engineering, particularly within the domain of power generation and renewable energy systems. Distinguished by its unique configuration featuring a wound rotor with external connections via slip rings as shown below in Figure II.10, this generator type offers unparalleled versatility and control over various operational parameters such as voltage, frequency, and reactive power. Through sophisticated control mechanisms, the wound rotor synchronous generator addresses critical challenges in grid integration of renewable energy sources by ensuring seamless synchronization with the grid and effective management of power fluctuations. Its adaptability and robust performance make it an indispensable asset in modern power systems, contributing significantly to the sustainable development of energy infrastructure worldwide [27].

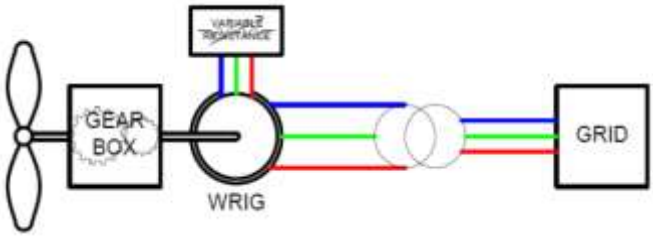

Fig II.10 Wound Rotor Synchronous Generator

II.4. Static Modelling of Doubly Fed Induction Generator

In this section, we will delve deeper into the complexities of the Doubly Fed Induction Generator (DFIG). Specifically, we will explore its modelling and control system to gain a comprehensive understanding of its operation and behaviour. Figure II.11 illustrates the primary configuration of a Doubly Fed Induction Generator (DFIG) coupled with a wind turbine. Typically, in conventional setups, the stator of the DFIG is directly linked to the grid. However, what sets DFIG apart from traditional systems is that its rotor is

connected to the grid via a partial-scale power converter. This unique arrangement enables the transmission of generated energy from both the stator and rotor, hence earning the designation "DFIG". While the majority of active power generated is transmitted to the grid through the stator, a fraction of the generated active power is channelled to the grid through the rotor [28].

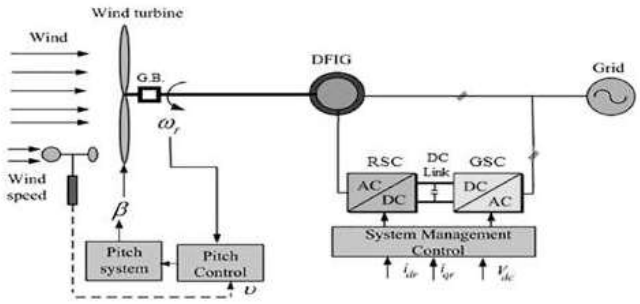

Fig II.11 Model Doubly Fed Induction Generator

II.4.1. DFIG Modelling Using an Arbitrary Reference Frame

Utilizing the d-q representation of an induction machine offers the potential for enhanced control flexibility. In the case of a Doubly Fed Induction Generator (DFIG), employing Park transformation on the conventional three-phase *abc* model allows for the formulation of a dynamic model within a d-q reference. Figures II.12a and II.13b show the equivalent circuit of the DFIG in the d-q frame. The stator and rotor voltages of the DFIG can be expressed as follows [29,30];

$$V_{ds} = R_s I_{ds} - \omega_s \psi_{qs} + \frac{\mathrm{d}\psi_{ds}}{\mathrm{dt}} \qquad (2.14)$$

$$V_{qs} = R_s I_{qs} + \omega_s \psi_{ds} + \frac{\mathrm{d}\psi_{qs}}{\mathrm{dt}} \qquad (2.15)$$

$$V_{dr} = R_r I_{dr} - (\omega_s - \omega_r)\psi_{qr} + \frac{\mathrm{d}\psi_{dr}}{\mathrm{dt}} \qquad (2.16)$$

$$V_{qr} = R_r I_{qr} + (\omega_s - \omega_r)\psi_{dr} + \frac{\mathrm{d}\psi_{qr}}{\mathrm{dt}} \qquad (2.17)$$

Where V_{ds}, V_{qs}, V_{qr}, V_{dr} are the d and q axis stator and rotor voltages, in (Volt), respectively. I_{ds} , I_{qs} , I_{dr} , I_{qr} are the d and q axis stator and rotor currents, in (Ampere), respectively. ψ_{ds} , ψ_{qs} , ψ_{dr} , ψ_{qr}r are the d and q axis stator and rotor fluxes, in (Wb), in the same order. R_s and R_r are the stator and rotor phase resistances, in (Ohm), respectively.

The flux equations for the stator and rotor can be written as follows;

$$\psi_{ds} = L_s I_{ds} + L_m I_{dr} \qquad (2.18)$$

$$\psi_{qs} = L_s I_{qs} + L_m I_{qr} \qquad (2.19)$$

$$\psi_{dr} = L_r I_{dr} + L_m I_{ds} \qquad (2.20)$$

$$\psi_{qr} = L_r I_{qr} + L_m I_{qs} \qquad (2.21)$$

Where L_s, L_m, and L_r denote the stator, mutual, and rotor inductances respectively, measured in Henry. Meanwhile, stator voltages maintain constancy in amplitude, frequency, and phase, while the stator flux ψ_s remains nearly constant. In the rotor-side controller, the d-axis of the rotating reference frame employed for d-q transformation aligns with the air-gap flux ψ_s, thus ψ_s=ψ_{ds}, $\psi_{qs} = 0$, and $d\psi_{qs}/dt = 0$. Given the stator flux ψ_{ds} is assumed constant, any change in ψ_{ds} is considered minute and hence negligible [28,29,30].

By substituting the above quantities in (5), (6) the stator currents can be written as:

$$I_{ds} = (\psi_{ds} - L_m I_{dr})/L_s \qquad (2.22)$$

$$I_{qs} = -(L_m L_s)/L_{qr} \qquad (2.23)$$

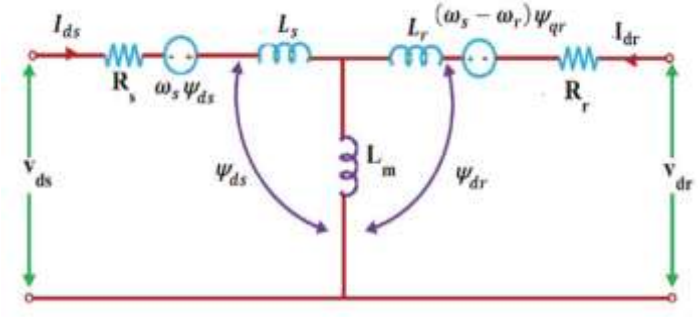

Fig II.12a equivalent circuits of DFIG in d-axis

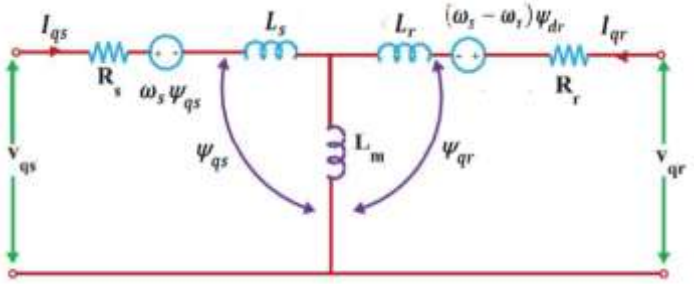

Fig II.12b equivalent circuits of DFIG in q-axis

As the value of the stator resistance (R_s) is considerably small compared to the stator reactance, so it can be neglected, V_{ds} is therefore as below;

$$V_{ds} = 0 \qquad (2.24)$$

$$V_{ds} = \omega_s \psi_{ds} \qquad (2.25)$$

With minimal power loses occurring in both the stator and rotor resistances, the resultant real and reactive power outputs from both the stator and rotor sides can be computed as:

$$P_s = \frac{3}{2}(V_{ds} I_{ds} + V_{qs} I_{qs}) = \frac{3}{2}\frac{Lm}{L_s}\omega_s \psi_{ds} I_{qr} \qquad (2.26)$$

$$Q_s = \frac{3}{2}(V_{qs} I_{ds} - V_{ds} I_{qs}) = \frac{3}{2L_s}\omega_s \psi_{ds}(\psi_{ds} - L_m I_{dr} \qquad (2.27)$$

$$P_R = \frac{3}{2}(V_{dr} I_{dr} + V_{qr} I_{qr}) \qquad (2.28)$$

$$Q_r = \frac{3}{2}(V_{qr} I_{dr} + V_{dr} I_{qr}) \qquad (2.29)$$

Where P_s , P_r represent stator-side and rotor-side power respectively. Q_s, Q_r are stator-side and rotor-side reactive power.

II.5. Conclusion

This chapter has covered the historical timeline of wind energy utilization, tracing its origins from ancient civilizations to the modern era. It highlights key milestones such as the development of the first electricity-generating wind turbines.

Additionally, the chapter explores the basics of wind turbine technology, including the classification of wind turbines into horizontal axis and vertical axis types. It provides detailed insights into the components of wind turbines, such as rotor blades, rotor hub, nacelle, generator, tower, and electronic components, showing their roles in wind energy conversion.

Furthermore, the chapter delves into the principles of wind power conversion, explaining the aerodynamic principles underlying wind energy conversion and the process of converting wind energy into mechanical and electrical energy.

This chapter offers a comprehensive understanding of wind power generation and the technologies involved, laying the groundwork for further exploration into wind energy systems and their applications.

CHAPTER III: TRANSIENT STABILITY ANALYSIS CONCEPT AND THEORY.

III.1. Introduction

III.1.1 Overview of Power System Stability

Power system stability refers to the ability of a power system to maintain a normal operating condition and stable equilibrium, or to return to an acceptable operating state after experiencing disturbances, whether small or large. Traditionally, instability issues in power systems are associated with maintaining the synchronism of machines within the system. However, instability can also occur without loss of synchronism, such as a sudden voltage drop due to a load change, which can destabilize the transmission line. The relative and absolute rotor angles, as well as the power angles between machines, are key indicators of system stability [25].

Disturbances in power systems can range from small, continuous changes like load variations to large, infrequent events such as generator trips or transmission line faults. Small disturbances are managed by the system's inherent ability to maintain acceptable voltage and frequency levels. Large disturbances, however, cause significant shifts in system parameters like voltage and frequency and trigger generation controls to restore the system to a normal or acceptable operating condition[31].

Power system stability is a complex and ongoing challenge for engineers worldwide. Previous foundational work has established a strong theoretical base for understanding stability issues. Modern approaches to solving stability problems involve understanding the scale of disturbances, modelling disturbance phenomena, and applying mathematical simulations. Advances in high-speed simulations and improved modelling of power system components, from protective devices to complex power generators, have significantly enhanced our ability to analyze and ensure reliable operation of the power network [31].

Due to the complexity of studying system stability in its entirety, power system stability has been categorized as shown in Figure III.1 to better understand and address specific stability issues. This categorization helps in developing targeted solutions to maintain reliable and stable power system operations.

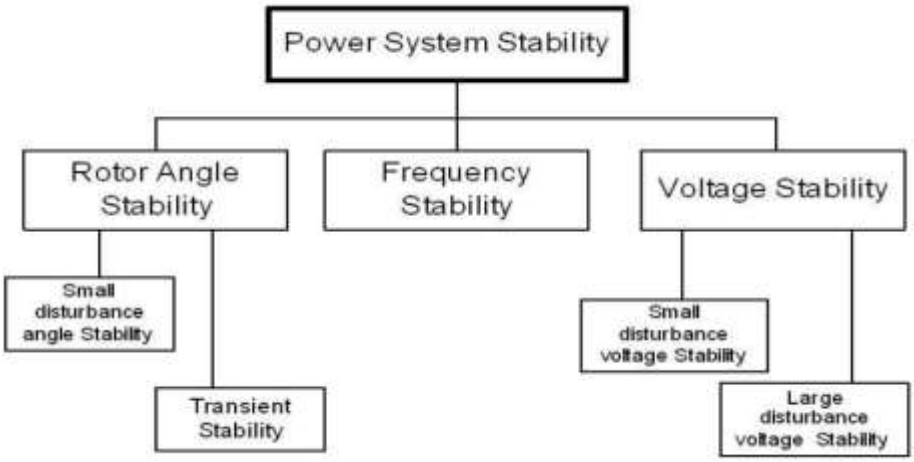

Fig III.1 Categories of power system[31]

III.1.2. Concept of Transient Stability Analysis

Transient stability analysis refers to the examination of a power system's capability to maintain angle stability following a significant disturbance, such as a short circuit on a transmission line or the disconnection of a generator [31]. It is a subset of rotor angle stability and focuses on ensuring the system's stability in the aftermath of large disturbances. Instability issues arising from transient events are typically aperiodic and stem from inadequate synchronizing torque. This analysis plays a crucial role in safeguarding the reliability and operability of power systems, particularly during disruptive events, by evaluating the system's ability to restore stability and prevent cascading failures [24].

It is crucial for ensuring the reliable operation of power systems, particularly in the presence of faults or disturbances. One key parameter used in this analysis is the critical clearing time (CCT), which represents the maximum duration between the occurrence of a fault and its clearance that allows the power system to regain stability [31].

Pai Wood [32] goes deeper on its assessment, often relying on time domain simulation, which involves solving the differential and algebraic equations governing the behaviour of power systems through a sequential computation method. Despite its effectiveness, this approach known for its computational intensity, primarily attributed to the complex nonlinear nature of transient stability analysis.

Stability determination can also employ the direct method, which relies on Lyapunov's second method. However, this approach is not widely used because of the difficulties in identifying a suitable Lyapunov function and establishing a practical stability domain [9,33].

Pattern recognition emerges as another method for transient stability analysis, drawing from past experiences to identify and apply relevant stability properties to current

scenarios. This approach uses historical data and observed patterns to inform stability assessments, providing valuable insights into system behaviour and potential stability risk [9].

III.2. Fundamentals of Transient Stability

III.2.1.Importance of Transient Stability Analysis in Wind Grids

Transient stability analysis plays a critical role in ensuring the reliable and secure operation of wind grid-connected systems. As wind energy continues to be integrated into power grids worldwide, understanding and mitigating transient stability issues become increasingly important. This section explores the significance of transient stability analysis in wind grids and its implications for grid reliability and performance.

- **Enhancing the Grid Resilience**

Transient stability analysis assesses how well wind grid-connected systems can handle sudden disruptions, like faults or sudden changes in how they operate. This analysis aids in understanding the system's capacity to withstand such disruptions and recover promptly, thereby contributing to the enhancement of grid resilience [34].

- **Grid Reliability**

Transient stability analysis helps grid operators evaluate the ability of wind energy systems to maintain stable operation during disturbances such as sudden changes in wind speed, faults, or switching events. This assessment enables operators to implement measures to enhance grid reliability and prevent cascading failures [35].

- **Integration Challenges**

Wind energy grids often face integration challenges due to the irregular nature of wind resources. Transient stability analysis allows operators to understand how fluctuations in wind power output affect grid stability, facilitating the development of strategies to manage these fluctuations effectively and maintain grid stability [10].

- **System Planning and Design**

During the planning and design phases of wind energy projects, transient stability analysis helps engineers assess the impact of wind power integration on grid stability and identify optimal locations for wind farms. Incorporating transient stability considerations into system planning enables the design of robust grid infrastructure capable of accommodating large-scale wind power integration [36].

- **Operational Decision Making**

Real-time transient stability analysis empowers grid operators to make informed decisions during normal and contingency operating conditions. By continuously

monitoring grid stability and predicting potential instability events, operators can take proactive measures to maintain grid stability, such as adjusting generation levels or activating grid support devices [9].

III.2.2. Challenges and Issues Associated with Transient Stability in Wind Grids

- **Wind Fluctuations**

Wind's changing nature makes wind grids less stable. Quick changes in wind speed and direction cause power output to fluctuate, which can make grids unstable. To fix this, smart strategies are needed to control the grid. These sudden changes make it hard to balance power supply and demand. As wind power grows, it's vital to keep grids stable despite these changes. Better forecasting and grid management help predict and handle wind changes, making wind power more reliable in grids [37].

- **Dynamic Behaviour of Wind Turbine**

Wind turbines demonstrate dynamic behaviour when responding to grid disturbances, playing a crucial role in maintaining transient stability. Turbine characteristics like inertia, control system response, and interaction dynamics with the grid significantly influence their ability to ensure stable operation during transient events. Understanding and optimizing these factors are important for enhancing the reliability and resilience of wind energy integration within power systems [38].

- **Grid Structure**

The topology and characteristics of the grid are pivotal factors influencing transient stability within wind grids. Weak grid connections and insufficient grid infrastructure can contribute to stability issues, particularly during transient events. Inadequate infrastructure may lead to voltage fluctuations, power imbalances, and increased susceptibility to disturbances, thereby posing significant challenges to the integration of wind energy into the grid. Addressing these grid structure concerns requires strategic planning and investment in grid reinforcement measures to ensure the reliable and resilient operation of wind energy systems within power grids [35].

- **Control Strategies**

The efficacy of control strategies implemented in wind turbines and grid-support functions play a critical role in shaping transient stability within wind grids. Optimization of control algorithms and coordination among wind turbines and other grid assets are indispensable for improving transient stability in these systems. By fine-tuning control mechanisms and ensuring seamless integration with grid operations, wind energy systems can better respond to transient events, thereby enhancing the reliability and resilience of power grids [21,38].

III.2.3 Techniques for Addressing Transient Challenges in Wind Turbine Operations

- **Pitch Control System**

A critical component in mitigating transients within wind turbine generators (WTGs) is the pitch control system. This system dynamically adjusts the angle of the turbine blades in response to fluctuating wind conditions. By precisely controlling the blade pitch, the system regulates both the rotor speed and the overall power output of the WTG. This dynamic adjustment is crucial for reducing transients. During sudden wind gusts, the pitch control system can quickly feather the blades, meaning it reduces the angle of attack of the wind on the blades. This effectively acts as a brake, preventing the rotor from over-speeding and experiencing excessive torque. Alternatively, when the wind slows down, the system adjusts the blade angle to catch more wind, ensuring the turbine generates maximum power. This dynamic response helps to dampen the impact of transient wind events, promoting smoother operation and enhancing the overall stability of the power grid [39,40].

- **Yaw control system**

While pitch control plays a vital role in mitigating transients, another crucial system contributes to overall stability, the yaw control system. Unlike pitch control, which focuses on adjusting the angle of attack of the blades, yaw control ensures the entire nacelle (the housing containing the gearbox, generator, and rotor) rotates to directly face the incoming wind. Maintaining proper alignment with the wind direction is essential for avoiding transients [40].

Sudden wind direction changes can cause the turbine to oscillate if not properly controlled. This can lead to transient-induced oscillations in rotor speed, torque, and power output. The yaw control system acts to counteract these disturbances by continuously monitoring wind direction sensors and adjusting the nacelle's orientation accordingly. By keeping the turbine aligned with the wind, the yaw control system minimizes the impact of these rapid directional shifts, reducing stress on turbine components and enhancing overall system stability [21].

- **FACTS (Flexible Alternating Current Transmission Systems)**

Advancements in power grid technology offer additional solutions to mitigate transients beyond the control systems within wind turbines themselves. Flexible Alternating Current Transmission Systems (FACTS) devices emerge as a powerful tool for enhancing transient stability within the broader power system. FACTS encompass a range of technologies designed to improve the controllability and flexibility of AC transmission. One prominent member of the FACTS family is the Static Synchronous Compensator (STATCOM). STATCOMs function by injecting or absorbing reactive power into the grid, dynamically adjusting parameters like voltage, impedance, and phase angle. This precise

control allows them to significantly improve the transmission capacity, stability, and overall reliability of the power system. In the context of transient stability, STATCOMs play a vital role in mitigating issues. During transients, rapid changes in power flow can cause voltage fluctuations and system oscillations. STATCOMs can act as a buffer, injecting or absorbing reactive power to regulate voltage levels and control power flow. This helps to dampen these oscillations and maintain system stability, preventing cascading failures and ensuring reliable power delivery [47].

III.3. Transient Stability Assessment Methods

In reviewing transient assessment methods, both classical and modern techniques play integral roles in analysing the stability of power systems during transient events. Classical methods, such as the Equal Area Criterion and Swing Equation, have long been foundational in transient stability analysis. The Equal Area Criterion evaluates stability by comparing the areas under the rotor angle versus time curve before and after a disturbance, while the Swing Equation describes the dynamics of synchronous generators' rotor angles.

Other methods such as Lyapunov Stability and Energy Function Analysis provide advanced insights into system stability. Lyapunov Stability quantifies a system's sensitivity to initial conditions, offering valuable information about its long-term behaviour. Energy Function Analysis evaluates stability by examining variations in system energy. Additionally, numerical methods like Euler, Modified Euler, Runge-Kutta, and Newton-Raphson among other methods are commonly used. By integrating these techniques, engineers can comprehensively assess transient stability, ensuring reliable and secure operation of power systems amid dynamic disturbances [35,33].

III.3.1. Classical methods

III.3.1.1. Swing Equations

In the world of power systems, Swing Equations are important tools for understanding how synchronous generators behave when they are all connected together. These equations show us how mechanical and electrical forces work together in the generators within the grid. The paths traced by these equations, called Swing curves, help us see how generator states change over time. By looking at these curves for all the generators, we can figure out if the system is stable or not and that is important for making sure it works well. For example, if we think about just one generator with its speed and the forces acting on it, those things really affect how well the generator works and how the whole system behaves. So, understanding Swing Equations is super important for making sure power networks run smoothly and efficiently [41].

Consider, for instance, a single synchronous generator characterized by its synchronous speed, $\omega s\, m$, and the pivotal electromagnetic and mechanical torques, Te and Tm , respectively. In the regime of steady-state operation;

T_a = T_m (3.1)

When a disturbance occurs, the torque deviates from steady state, causing an accelerating (Tm >Te) or decelerating (Tm <Te) torque.

T_a (accelerating torque) = T_m – T_e (3.2)

Assume J is the combined inertia of generator and prime mover, neglecting friction and damping torque, we have:

J θ_m'' = T_a = T_m – T_e (3.3)

where θ is the angular displacement of the rotor relative to the stator, the suffix m means generator. The rotor speed relative to synchronous speed is given by:

θ_m = $\omega\, s\, s$ t + $\delta\, m$ (3.4)

From equation (3.4), we obtain the angular speed of the rotor:

ω_m = θ_m' = $\omega_{sm} t + \delta_m$' (3.4)

Where

θ_m'' = δ_m'' (3.5)

Substituting (3.6) into (3.3), we obtain

J δ_m'' = Ta = Tm - Te (3.6)

Multiply eq. (2.7) by :

ω_m J δ_m''= ω_m Tm - ω_m Te = Pm - Pe (3.7)

J ω_m is called the constant of inertia, referenced by "M" and associated with Wk (kinetic energy):

W_k= 0.5 Jω_m^2 = 0.5Mω_m (3.8)

or

M = (2W_k/ω_{sm}) (3.9)

For small changes ω_m, it is reasonable to assume that M is constant, so

M= (2W_k)/ (ω_{sm})

Then we obtain the standard from of the swing equation:

M δ_m'' = Pm – Pe (3.10)

III.3.1.2. Equal Area Criterion

The Equal Area Criterion stands as a fundamental technique in transient stability analysis, particularly for assessing the stability of two-machine systems or a single machine interfacing with an infinite bus. Unlike methods reliant on the swing equation, this graphical approach determines stability conditions by balancing areas on the power angle diagram between the P-curve and the updated power transfer line. The criterion evaluates the energy exchange during transient states: Area A1 symbolises the rotor's stored kinetic energy during acceleration, while A2 represents the energy transferred to the system during deceleration. Stability lies on A1 exceeding A2 for positive areas (indicating generation action) and A2 surpassing A1 for negative areas (shows stable operation). Moreover, the Equal Area Criterion sets limits on system load capacity, ensuring stability by equating areas under the mechanical and electrical power curves. Challenges to transient stability stem from sudden load changes, line disconnections altering system reactance, and faults necessitating rapid response and post-fault analysis. Addressing these, the method involves plotting power angle curves under various conditions, determining initial angles δo, and using the criterion to find out new displacement angles δ, which helps determine the maximum allowable angles and the loads they correspond to [42,33].

Where $P_a = P_m - P_e$ accelerating power and δ is the initial power angle before the rotor begins to swing because of a disturbance. The stability ($\frac{d\delta}{dt} = 0$) criterion implies that;

$$\int_{\delta_0}^{\delta} \mathrm{P_a d}\delta = 0 \qquad (3.11)$$

For stability, the area under the graph of accelerating power versus δ must be zero for some value of δ; i.e., the positive (accelerating) area under the graph must be equal to the negative (decelerating) area. This criterion is therefore known as the equal area criterion for stability and is shown by the power-angle relationship and rotor angle-time diagram in Figure III.2.

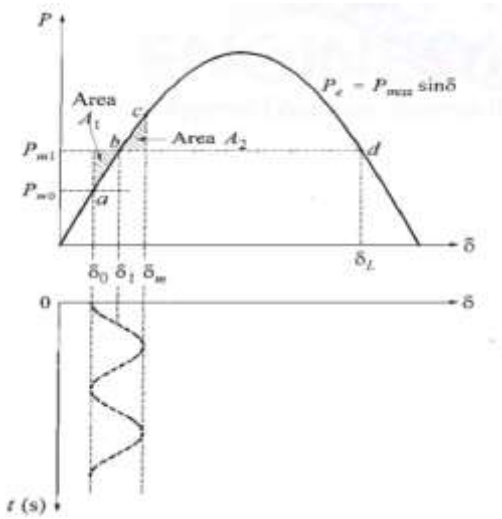

Fig III.2 Equal area criterion

III.3.2. Numerical methods

Among various numerical methods, the 4th order Runge-Kutta method is widely used to assess transient stability in power systems. This method is a numerical integration technique that operates by iteratively calculating the state variables of a dynamic system at discrete time steps. It estimates the state variables by considering the system's behaviour slopes at multiple points within each time step. By computing intermediate slopes at different points and combining them using a weighted average, the Runge-Kutta 4th order method achieves greater accuracy and stability compared to lower-order methods. This makes it particularly reliable for simulating the dynamic behaviour of power systems following disturbances.

In the context of transient stability analysis of power systems, the Runge-Kutta 4th order method is a valuable tool for simulating the system's dynamic response to disturbances such as faults, load changes, or switching events. By discretizing the differential equations that govern the dynamics of generators, loads, and network components, engineers can employ this method to predict the evolution of system variables such as rotor angles, voltages, and currents over time. Solving the swing equation, which describes the dynamic behaviour of synchronous generators, typically involves rewriting it as a set of first-order differential equations. This approach facilitates the simulation of both single-machine and multi-machine systems, with iterations performed per time step in the case of multiple machines [33].

The swing equation given in previous section can be written as a set of two first order differential equations as follows:

$$\frac{d\delta}{d\mathrm{t}} = \omega - \omega_s \qquad (3.12)$$

$$\frac{d\omega}{d\mathrm{t}} = \frac{\pi \mathrm{f}}{H}\mathrm{P}_m - \mathrm{P}_e$$

$P\,m$ is the mechanical power input to the machine and $P\,e$ is the electrical power output. The RK4 method uses four estimations where h denotes the integration time step. The first estimation is shown in Equation (3.13):

$$\mathrm{K1}_\delta = h(\omega - \omega_s)$$
$$\mathrm{K1}_\omega = h(\frac{\pi \mathrm{f}}{H}\mathrm{P}_m - \mathrm{P}_e) \quad (3.13)$$

The second approximation is given by Equation (3.14):

$$\mathrm{K2}_\delta = h(\omega + \frac{\mathrm{K1}_\omega}{2} - \omega_s)$$
$$\mathrm{K2}_\omega = h(\frac{\pi \mathrm{f}}{H}\mathrm{P}_m - \mathrm{P}_e) \quad (3.14)$$

The third approximation is given by Equation (3.15):

$$\mathrm{K3}_\delta = h(\omega + \frac{\mathrm{K2}_\omega}{2} - \omega_s)$$
$$\mathrm{K3}_\omega = h(\frac{\pi \mathrm{f}}{H}\mathrm{P}_m - \mathrm{P}_e) \quad (3.15)$$

The fourth approximation is given by Equation:

$$\mathrm{K4}_\delta = h(\omega + \mathrm{K3}_\omega - \omega_s)$$
$$\mathrm{K4}_\omega = h(\frac{\pi \mathrm{f}}{H}\mathrm{P}_m - \mathrm{P}_e) \quad (3.16)$$

These approximations are used to calculate the angular velocity and the rotor angle for the next time step as shown in Equations:

$$\omega_{n+1} = \omega_n + \frac{1}{6}(\mathrm{K1}_\omega + 2\mathrm{K2}_\omega + 2\mathrm{K3}_\omega + \mathrm{K4}_\omega)$$
$$\delta_{n+1} = \delta_n + \frac{1}{6}(\mathrm{K1}_\delta + 2\mathrm{K2}_\delta + 2\mathrm{K3}_\delta + \mathrm{K4}_\delta) \quad (3.17)$$

III.4. Models

III.4.1. DFIG control models

III.4.1.1. Grid Side Control

Figure III.3 illustrates the overall structure of the GSC system. The primary objectives of a grid side control is to regulate the DC link voltage and control the active and reactive

power (P_{GSC}, Q_{GSC}) delivered to the grid by manipulating the phase currents through two current control loops. The regulation of active power is directly related to the control of the DC bus voltage. To manage the GSC powers P_{GSC} and Q_{GSC}, we implement a grid voltage vector orientation control (VOC). This method maintains the grid voltage vector V_s aligned with the q-axis ($V_{ds} = U_s$, $V_{ds} = 0$). We give the expression of the GSC powers according to the GSC currents as follows [38]:

$$P_{GSC} = U_S I_{qf} \qquad (3.18)$$
$$Q_{GSC} = U_S I_{df} \qquad (3.19)$$

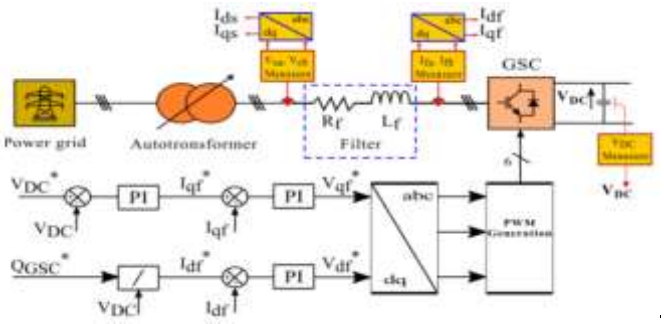

Fig III.3 Grid Side Control

The decoupled model obtained allows controlling the GSC powers independently. For the GSC active power P_{GSC} control, we act on GSC quadrature current I_{qf} and we act on the GSC direct current I_{df} for GSC reactive power control. The GSC voltages references, which are the outputs of the current controllers, are given as follows:

$$V_{df} = R_f I_{df} + L_f \frac{dI_{df}}{\mathrm{dt}} - \omega_s L_f I_{qf} \qquad (3.20)$$
$$V_{qf} = R_f I_{qf} + L_f \frac{dI_{qf}}{\mathrm{dt}} + \omega_s L_f I_{df} + U_s \qquad (3.21)$$

Where R_f, L_f represent filter resistance and filter inductance respectively. V_{df} and V_{qf} are the GSC voltages.

III.4.1.2. Rotor Side Control

Rotor side DFIG is connected to grid through bi-directional AC-DC-AC converters. The main function of rotor side control is to achieve decoupled control of active and reactive power. Rotor voltage can be modified as a function of rotor currents and stator flux [43]:

$$V_{dr} = R_r i_{dr} + \sigma L_r \frac{\mathrm{d}}{\mathrm{dt}} i_{dr} - \omega_r \sigma L_r i_{qr} + \frac{L_m}{L_r} \frac{\mathrm{d}}{\mathrm{dt}} \psi_s \qquad (3.21)$$
$$V_{qr} = R_r i_{qr} + \sigma L_r \frac{\mathrm{d}}{\mathrm{dt}} i_{dr} + \omega_r \sigma L_r i_{dr} + \omega_r \frac{L_m}{L_r} \frac{\mathrm{d}}{\mathrm{dt}} \psi_s \qquad (3.22)$$

In normal operation, the stator flux, ψ_s remains constant as the stator is directly connected to the grid at a constant AC voltage, resulting in $\frac{\mathrm{d}}{\mathrm{dt}}\psi_s = 0$. Equations (3.21) and (3.22) show that rotor current control can be achieved by employing a PI controller for each current component, with cross terms included at the output of each regulator to aid control. Once the current control loops and flux angle calculation are understood, the complete control system can be implemented. Since the d-axis of the reference frame aligns with the stator flux space vector, the torque expression simplifies as follows:

$$T_{em} = \frac{3}{2}p\frac{L_m}{L_s}(\omega_{qs} - \psi_{ds}\mathrm{i}_{qr}) \quad \Rightarrow T_{em} = \frac{3}{2}p\frac{L_m}{L_s}\psi_s\mathrm{i}_{qr} \quad \Rightarrow T_{em} = \mathrm{K}_T\mathrm{i}_{qr} \qquad (3.23)$$

In a similar way, by developing the stator reactive power Q_s expression in the frame, we obtain:

$$Q_s = \frac{3}{2}(v_{qs}i_{ds} - v_{ds}\mathrm{i}_{qs}) \quad \Rightarrow Q_s = -\frac{3}{2}\omega_s\frac{L_m}{L_s}(i_{ds} - \frac{\psi_s}{L_m}) \quad \Rightarrow Q_s = K_Q(i_{ds} - \frac{\psi_s}{L_m}) \qquad (3.24)$$

Therefore, because of the orientation chosen, it can be seen that both rotor current components independently allow us to control the torque and reactive stator power. In this way, based on above expressions, Figure III.4 illustrates the complete vector control of the DFIG.

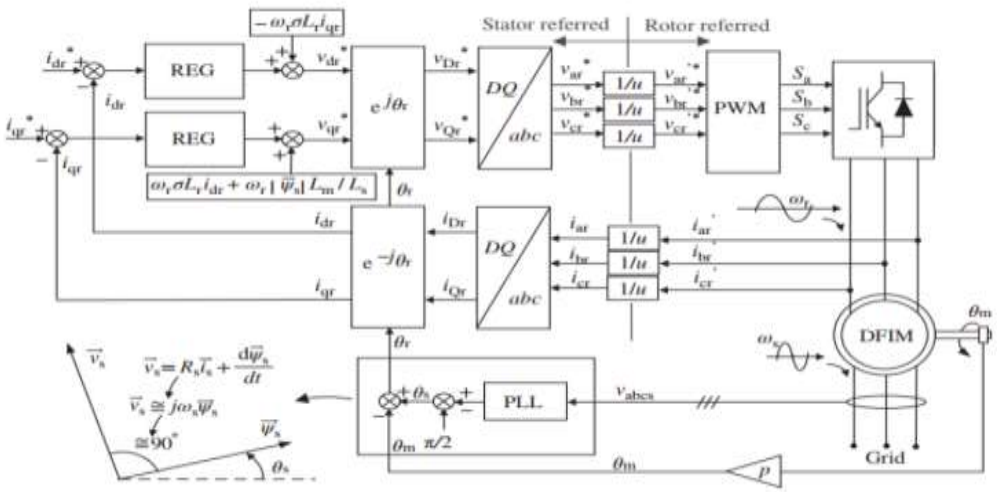

Fig III.4 Rotor Side Control in DFIG[43]

III.4.2. Dynamic Model of Wind Turbine Drivetrain

The primary function of the wind turbine's gearbox is to transform the low rotational speed and high torque of the rotor shaft, known as the low speed shaft (LSS), into higher speed and lower output torque on the high-speed shaft (HSS), which is necessary to power the generator. This transformation is achieved through multiple gear stages. The

varying torque of the rotor serves as an input to the gearbox, subjecting each component of the wind turbine generator (WTG) to significant transient loads, often absorbed by the gears and bearings. The specific configuration of the gearbox depends on the desired output speed for the generator. The conversion of energy from the wind domain to the mechanical domain is a multidisciplinary process that involves aerodynamics, fluid mechanics, and other disciplines. For simplicity and ease, it is defined as follows [14]:

$$P_w = \frac{1}{2}\rho_{air}\pi R^2 C_p v^3 \qquad (3.25)$$

Setting up the aerodynamic model is mainly for the purpose of supplying mechanical torque to the shafting model. As a result, the torque equivalent equation is given as:

$$T_w = \frac{P_w}{\omega_t} \qquad (3.26)$$

Where:

P_w is the mechanical power obtained from the wind, T_w is the mechanical torque transformed from the energy extracted from the wind by the turbine, ω_t is the turbine's angular speed, ρ is the density of the air, R is the radius of the wind wheel, v represents the corresponding speed of the wind, C_p is the wind energy utilization coefficient, determined by both the tip speed ratio λ and the pitch angle β.

Different methods exist for modelling the shafting in DFIG-based wind turbines, leading to two main types: those employing two masses and those employing three masses. Both models utilize mechanical torque and electromagnetic torque as input variables. Currently, the two-mass block model is preferred by researchers. The mechanical shaft assembly of a DFIG-based wind turbine consists of components such as the rotor, low-speed drive shaft, high-speed drive shaft, and generator. In the two-mass block model, the turbine itself constitutes one mass block, while the generator and gearbox together form another. Figure III.5 shows a typical dynamic model of a wind turbine drivetrain [44].

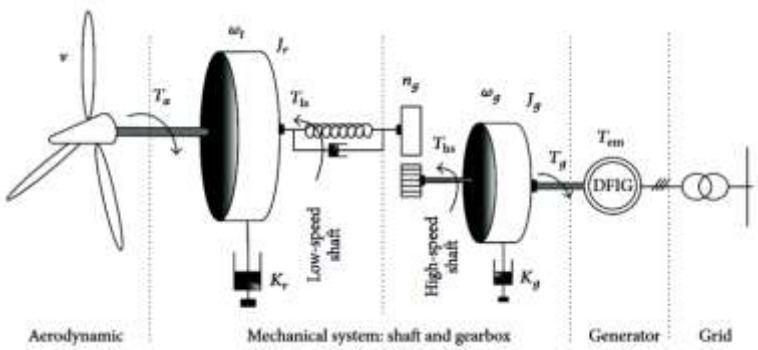

Fig III.5 Dynamic Model of Wind Turbine Drivetrain

The motion equations of the whole system in the case of the 2-mass block model of shafting are given by the following equations:

$$2H_t \frac{\mathrm{d}\omega_t}{\mathrm{dt}} = T_w - T_{shaft} - D_t\omega_t \qquad (3.28)$$

$$2H_g \frac{\mathrm{d}\omega_g}{\mathrm{dt}} = T_{shaft} - T_e - D_g\omega_g \qquad (3.29)$$

$$\frac{\mathrm{d}\theta_s}{\mathrm{dt}} = \omega_0(\omega_t - \omega_g) \qquad (3.30)$$

$$T_{shaft} = K_s\theta_s + D_s(\omega_t - \omega_{g)} \qquad (3.31)$$

Where: H_t is the turbine's inertia time constant, H_g is the generator's inertia time constant, ω_t is the turbine speed, ω_g is the generator speed, K_s is the shaft's stiffness coefficient, θ_s is the relative angular displacement (shaft's torsional angle). D_t, D_g, D_s are the torsional damping coefficients for transmission shaft, turbine rotor, and generator rotor respectively. T_w is the turbine's input mechanical torque and T_e is the generator's electromagnetic torque.

III.4.3. The Dynamic Model of DFIG

The drive train's function is to transform the aerodynamic torque generated by the wind into mechanical torque on the low-speed shaft, which connects to the generator via a gearbox. The gearbox is assumed to be frictionless and has a gear ratio of 1: n. Two types of torques act upon the turbine: the accelerating torque from the wind (T_m), which represents the mechanical torque applied to the rotor, and the decelerating electrical torque (T_e), which is the electromagnetic torque applied to the rotor by the generator. The power flow is shown in Figure III.6. The output power of the wind turbine (P_m) serves as the input power of the Doubly Fed Induction Generator (DFIG), which converts this power into electrical power to supply the grid through both the stator and rotor sides [21,29].

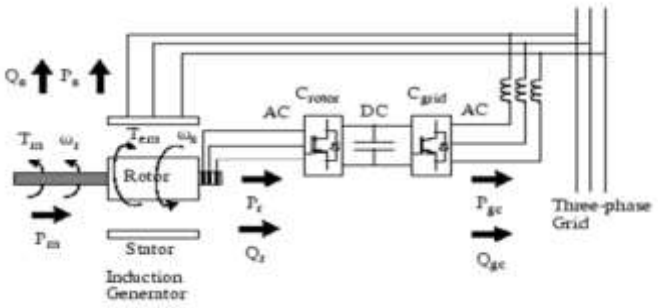

Fig III.6 Dynamic Model of DFIG[29]

The slip of generator obtained by equation

$$S = \frac{\omega_s - \omega_r}{\omega_s} \qquad (3.32)$$

Where ω_s : synchronous speed ω_r : rotational speed of rotor

$$P_m = T_m \omega_r \quad (3.33)$$

$$P_s = T_e \omega_s \quad (3.34)$$

$$J \frac{\mathrm{d}\omega_r}{\mathrm{dt}} = T_m - T_e \quad (3.35)$$

Where P_m is the output mechanical power of the turbine and P_s is the stator output power of the DFIG.P_r is the rotor output power of the DFIG and J is moment of inertia.

In steady-state at fixed speed for a loss less generator $T_e = T_m$ and $P_m = P_s + P_r$ hence;

$$P_r = P_m - P_s = T_m \omega_r - T_e \omega_s = -T_m (\frac{\omega_s - \omega_r}{\omega_s}) \omega_s$$

$$-sT_m \omega_s = -\mathrm{s}P_s \quad (3.36)$$

The total real output power of the DFIG is given by:

$$P_t = P_s + P_r = P_s - \mathrm{s}P_s = P_s(1\text{- s}) \quad (3.36)$$

This equation illustrates the power flow or slip power of the Doubly Fed Induction Generator (DFIG). The rotor power is contingent upon the slip, thus the DFIG operates either in sub-synchronous mode (where the rotor speed is less than the synchronous speed of the supply) or super-synchronous mode (where the rotor speed exceeds that of the supply). In both modes, the slip power can flow in either direction: from the supply to the rotor in super-synchronous mode or from the rotor to the supply in sub-synchronous mode.

III.4.4. The MATLAB Simulation Model of DFIG

Figure III.7 shows a doubly-fed induction generator (DFIG) consisting of a wound rotor induction generator and an AC/DC/AC IGBT-based PWM converter modelled by voltage sources. The stator winding is connected directly to the grid while the rotor is fed at variable frequency through the AC/DC/AC converter. The DFIG technology allows extracting maximum energy from the wind for low wind speeds by optimizing the turbine speed, while minimizing mechanical stresses on the turbine during gusts of wind [47].

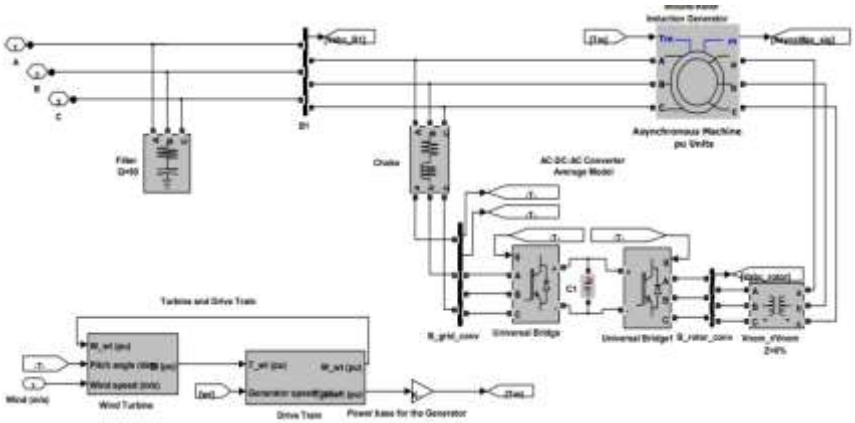

Fig III.7 MATLAB Simulation Model of DFIG

III.4.5. Power Stability Analysis Model of IEEE 9-bus system

To effectively study the transient stability of a conventional power grid, previous research has often used IEEE bus systems integrating them with different renewable energy systems. Stability studies require an understanding of the prefault network load flow data. Figure III.8 shows a typical model of a standard IEEE 9-bus system. This system includes one swing bus, two generator PV buses, and six load PQ buses.

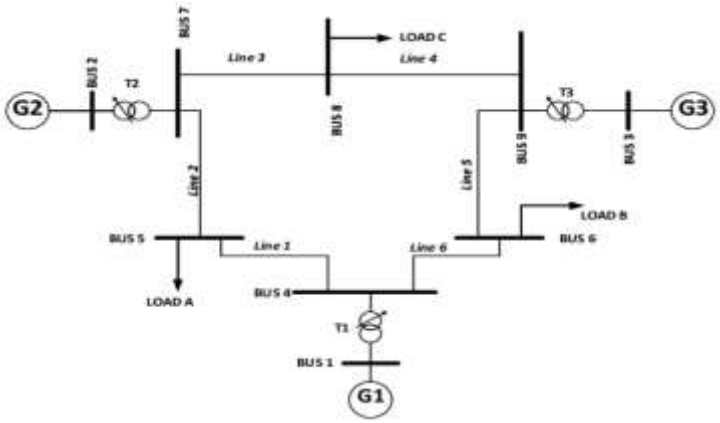

Fig III.8 IEEE9 bus network [46].

III.4.5.1 Parameters of 9-bus system

Table III.1: Transmission line data

Line From	Line To	Resistance R (pu)	Reactance X (pu)	Susceptance B (pu)
1	4	0.0000	0.0576	0.000
2	7	0.0000	0.6250	0.000
3	9	0.0000	0.0586	0.000
4	5	0.0100	0.0850	0.176
5	6	0.0170	0.0920	0.158
6	5	0.0320	0.1610	0.306
7	8	0.0085	0.0720	0.149
8	8	0.0119	0.1008	0.209
9	6	0.0390	0.1700	0.358

Table III.2: Bus data

Bus number	Bus type	Bus voltage(Kv)	Bus voltage(pu)	Angle(deg)	Generator	Generator	Load	Load
					P(MW)	Q(MVar)	P(MW)	Q(MVar)
1	Slack	16.5	1.040	0	247.5	0	0	0
2	PV	18	1.025	0	163	0	0	0
3	PV	13.8	1.025	0	85	0	0	0
4	PQ	230	1	0	0	0	0	0
5	PQ	230	1	0	0	50	125	50
6	PQ	230	1	0	0	30	90	30
7	PQ	230	1	0	0	0	0	0
8	PQ	230	1	0	0	35	100	35
9	PQ	230	1	0	0	0	0	0

Integrating renewable energy sources into the IEEE 9-Bus system can be achieved through various methods. This study illustrates one approach by connecting a wind farm at bus 10 to the grid at bus 7 using a 230 kV transmission line. A step-up transformer is utilized to facilitate this interconnection, demonstrating the system's adaptability for diverse renewable energy integration.

III.5. Conclusion

This chapter has provided a comprehensive exploration of transient stability analysis, emphasizing its critical role in ensuring the reliability and security of wind grid-connected power systems. By examining the dynamic responses of power systems to significant disturbances, transient stability analysis offers valuable insights into maintaining angle stability and preventing cascading failures. Various methods, including classical approaches like the Equal Area Criterion and Swing Equations, as well as direct methods such as the Runge-Kutta 4th order method, were discussed for their contributions to stability assessments.

Furthermore, the chapter highlighted the unique challenges associated with wind energy integration, such as fluctuating wind conditions and dynamic turbine behaviour, and underscored the importance of advanced control strategies, like pitch and yaw control systems, in mitigating transient instability. Through detailed discussions on the dynamic modelling of wind turbine drivetrains and DFIG control mechanisms, this chapter provided a robust framework for understanding and addressing the transient stability challenges in wind energy systems. Ultimately, integrating these analytical and control methodologies into system planning, design, and operation is paramount for enhancing the resilience and reliability of modern power grids as they increasingly incorporate renewable energy sources.

CHAPTER IV: SIMULATION AND RESULTS

IV.4.1. Introduction

In this section, a comprehensive transient stability analysis was conducted by connecting a wind farm, comprising 34 turbines each rated at 1.5 MW, to an IEEE 9-bus grid system. Three different cases were simulated and compared to effectively understand the resulting changes:

1. Simulation of the wind farm,
2. Simulation of the IEEE 9-bus grid system,
3. Simulation of the IEEE 9-bus grid system integrated with a wind farm.

The CCT, which refer to the durations necessary to detect, isolate, and eliminate faults to restore stability and continuity of the power supply[31], are used to understand how the grid responds to faults. Accurately determining these critical times is essential to minimizing system disruptions and ensuring the safety and reliability of the power supply.

IV.4.2. Case 1: Simulation of the wind farm

Figure IV.1 outlines the model of a wind farm using the doubly fed induction generators with a capacity of 51 MW comprising of thirty-four 1.5 MW wind turbines linked to a 25 kV distribution system. These turbines feed power into a 230 kV grid through a 30 km line, 25 kV feeder.

Utilizing doubly fed induction generator (DFIG) technology, each turbine integrates a wound rotor induction generator and an AC/DC/AC IGBT-based PWM converter represented by voltage sources. The stator winding is directly connected to the 60 Hz grid, while the rotor receives variable frequency input through the AC/DC/AC converter. DFIG technology optimizes turbine speed to maximize energy extraction from low wind speeds while minimizing mechanical stresses during gusts.

During the demonstration, wind speed is held constant at 15 m/s. A torque controller is employed in the control system to maintain speed at 1.2 pu, while reactive power production by the turbine is regulated at 0 MVar.

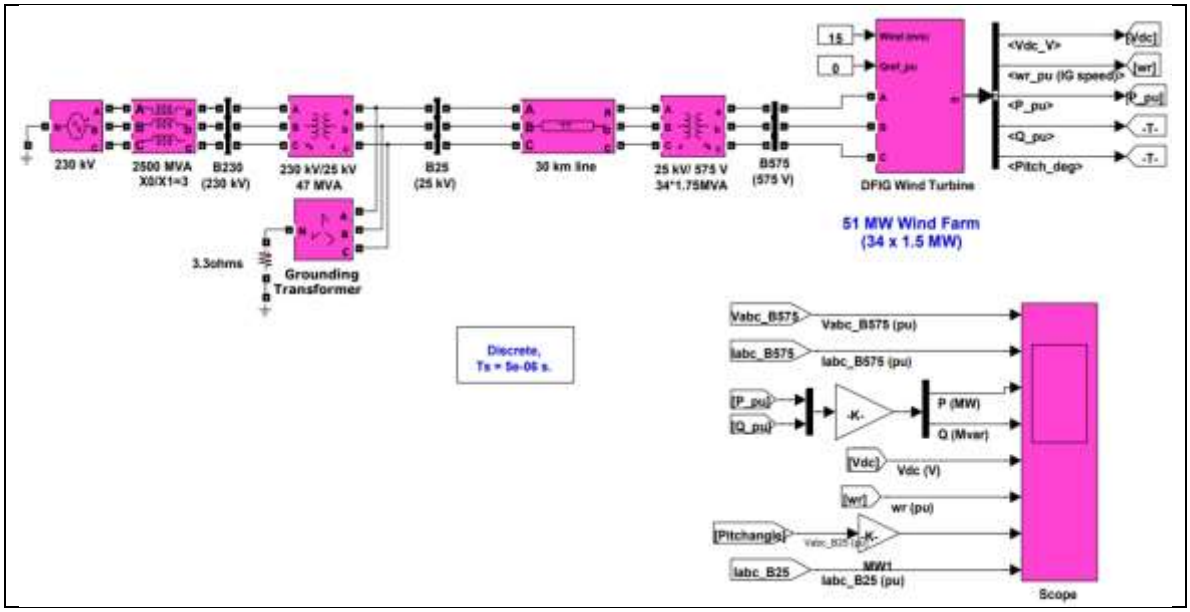

Fig IV.1 Simulink model of a wind farm

IV.4.2.1. Discussion

In this analysis, we represented Simulation 1 for a period of 10 seconds. We utilized graphs to illustrate the rotational speed, rotor angle, active power and DC link capacitor voltage of wind turbines. Most of these metrics are scaled using per unit (pu) values, with the base power being the nominal power of each wind turbine (1.5 MW), and 1 p.u signifying the turbine's nominal power.

We started by examining two crucial mechanical parameters: the rotational speed and rotor angle of the wind turbine. The rotor's rotational speed is controlled by adjusting the blade angle. After an initial disturbance, the rotor angle exhibits oscillations, settling down after 3 seconds, indicating system stability as shown in Fig IV.2a. Furthermore, the rotational speed, shown in Figure IV.2b, starts at 1.2 pu but subsequently oscillates to values more and less than the initial speed for 3 seconds. This suggests that the wind turbine's generator rotor no longer rotates at its rated speed, showcasing the strong dependence of rotational speed on wind power.

Figure IV.2c illustrates small fluctuations in the DC link capacitor voltage, influenced by variations in rotor active power and output power due to changes in wind speed. Additionally, Figure IV.2d demonstrates that the wind farm's DC voltage is the cumulative sum of individual turbine DC voltages. This implies that the Grid Side Converter (GSC) maintains the wind farm's DC voltage at a constant value, ensuring active power exchange between the generator and the grid. Figures IV.2e and IV.2f display the initial fluctuations in the active and reactive power output of the wind farm, which stabilize after approximately 3 seconds. These fluctuations illustrate the variations in power generation during the simulation period and highlight the dependence on wind power applied to turn the rotor.

Lastly, verifying the DC voltage is important to ensure the flawless operation of our wind farm.

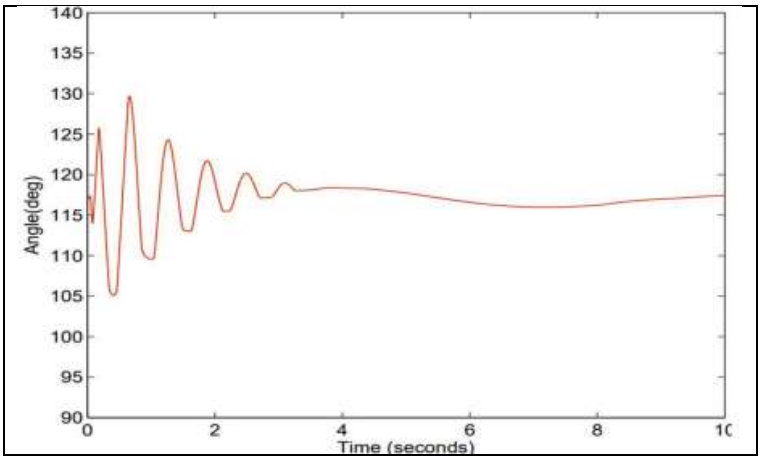

Fig IV.2a Rotor Angle

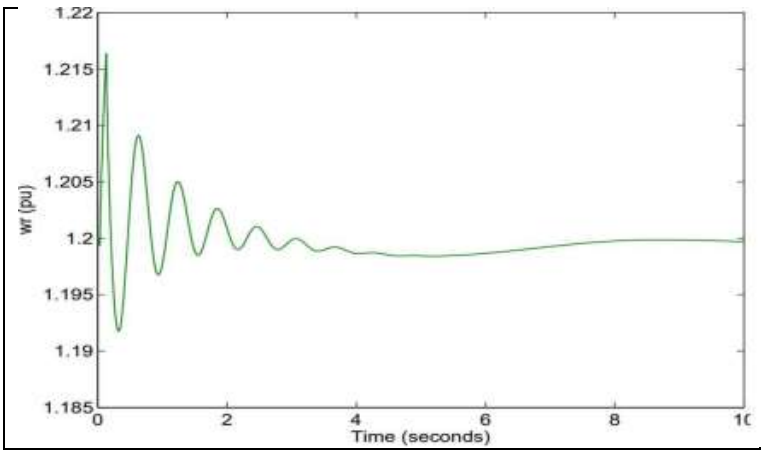

Fig IV.2b Rotor Speed

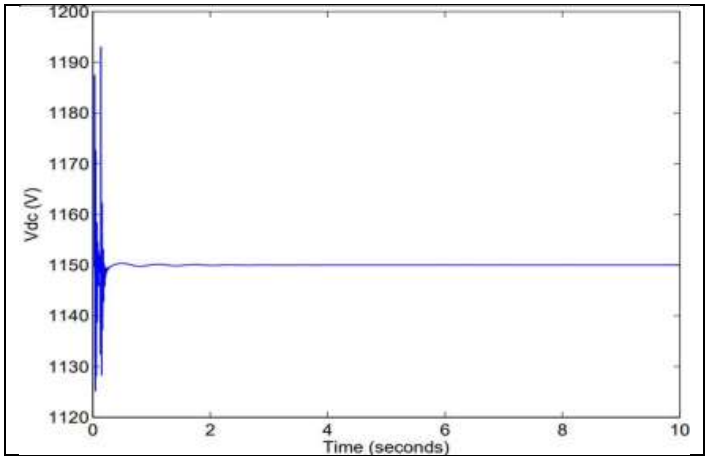

Fig IV.2c DC Link voltage

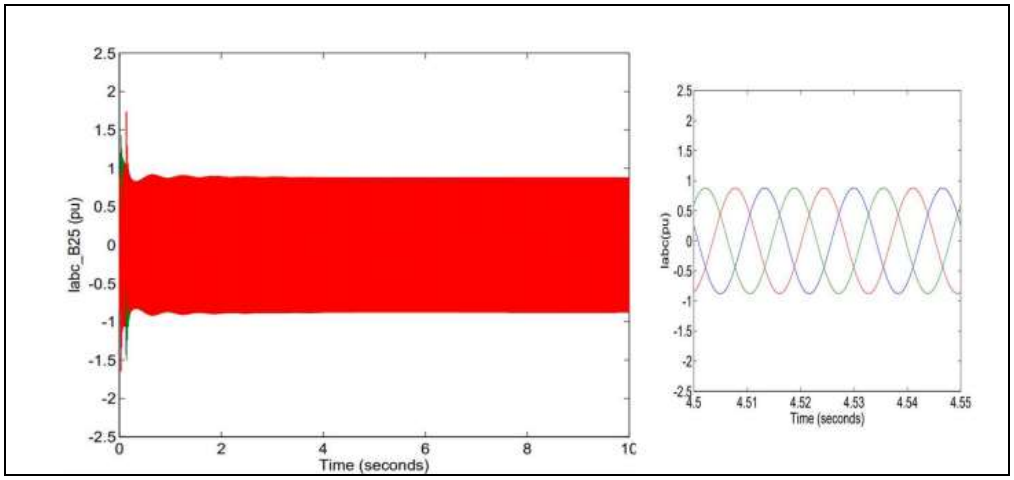

Fig IV.2d Three Phase voltage

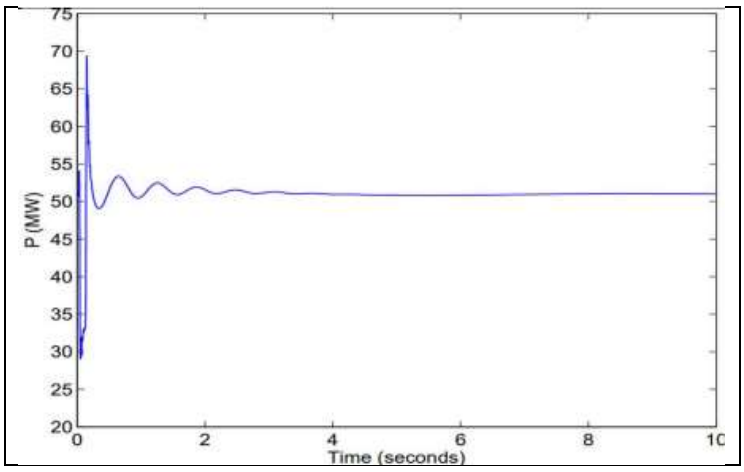

Fig IV.2e Active Power

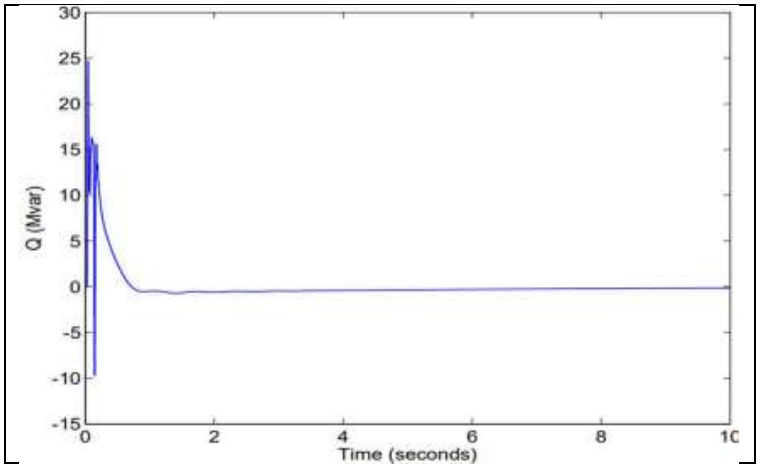

Fig IV.2f Reactive Power

After simulating the wind farm, it was observed that the system effectively responded to varying wind inputs, maintaining stable electrical output and demonstrating the robustness and reliability of the DFIG in managing grid stability under fluctuating conditions.

IV.4.3. Case 2: Simulation of the IEEE 9-bus grid system

The IEEE9 Bus system in this section was analysed for the study of its transient stability. It was modelled in Simulink as shown in Figure IV.3. The base power of the network is 100MVA and the frequency is 60HZ. The simulated load flow parameters are given in Figure IV.4 with:
Vbase = 230KV,Sbase = 100MVA,Zbase=529ohms.

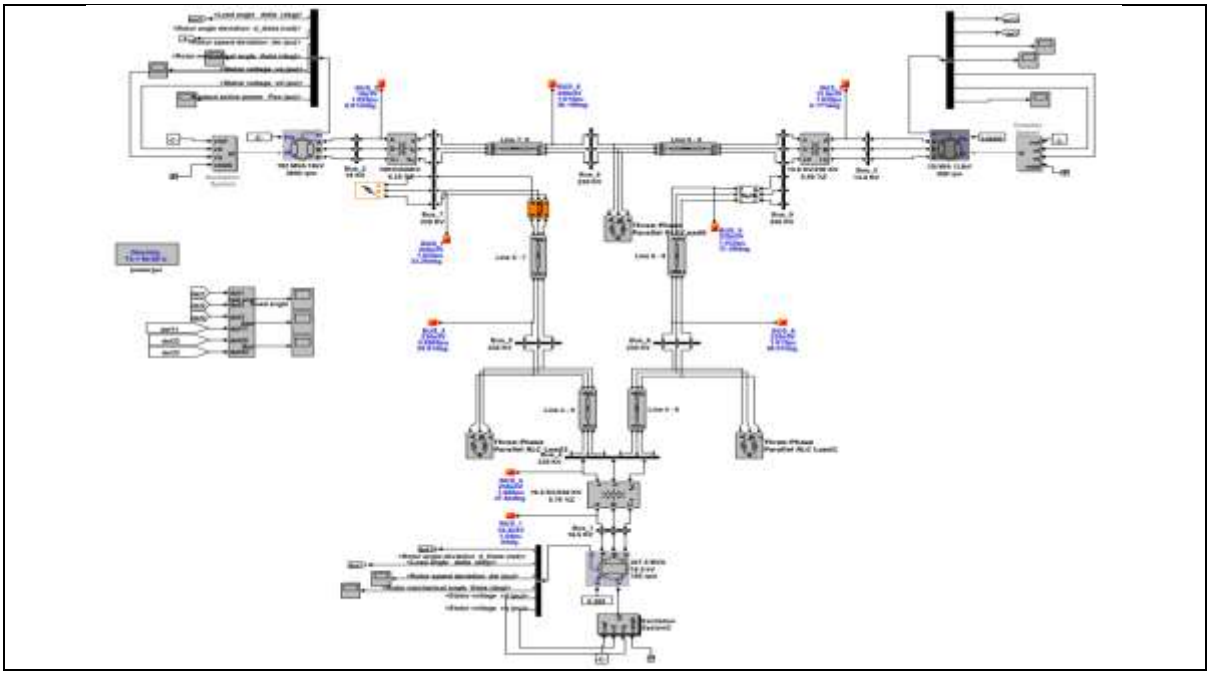

Fig IV.3 Simulation Model of IEEE 9-Bus System

Table IV.1: Load flow analysis of IEEE 9-Bus System model

Bus Number	Bus Name kV	PGen(MW)	QGen(MVar)	V_LF(pu)	Vangle(deg)	P_LF(MW)	Q_LF(MVar)
1_Vrsc Swing	Bus_1 16.50	0	0	1.0141	0.00	72.19	25.80
2	Bus_4 230	0	0	1.0261	-2.23	0.00	0.00
3_RLC Load PQ	Bus_5 230	125	50	0.9962	-4.00	125	50.00
4_RLC Load PQ	Bus_6 230	90	30	1.0131	-3.70	90.00	30.00
5	Bus_7 230	0	0	1.0259	3.62	0.00	0.00
6	Bus_9 230	0	0	1.0324	1.87	0.00	0.00
7_RLC Load PQ	Bus_8 230	100	35	1.0160	0.63	100.00	35.00
8_Vsrc PV	Bus_2 230	163	0	1.0250	9.17	163.00	6.69
9 _Vsrc PV	Bus_3 230	85	0	1.0250	4.56	85.00	-10.78

IV.4.3.1. Discussion

In this setup, it was analysed to simulate classical transient stability analysis examples [25]. A three-phase fault was simulated at bus 7, followed by clearing the fault by opening the line between buses 7 and 5 after 0.36 seconds. The absolute rotor angles of

all generators, as well as the relative rotor angles of generators 2 and 3 with respect to generator 1, are plotted in Figures IV.4a and IV.4c. A small difference in swing limits and time variations can be observed in the rotor angle plots compared to the classical example results shown in Figures IV.4b and IV.4d. This difference is because the Simulink machine model is more detailed and the simulations start at different times.

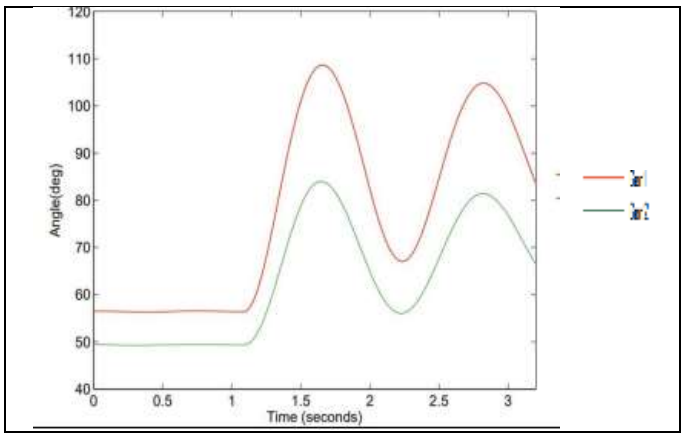

Fig IV.4a Relative angle plot of all generators with respect(w.r.t) G1

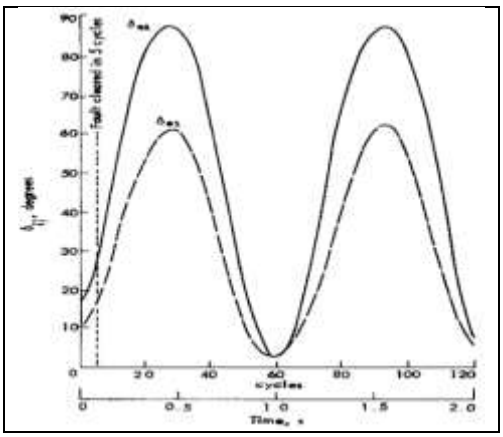

Fig IV.4b Classical example of Relative angle plot

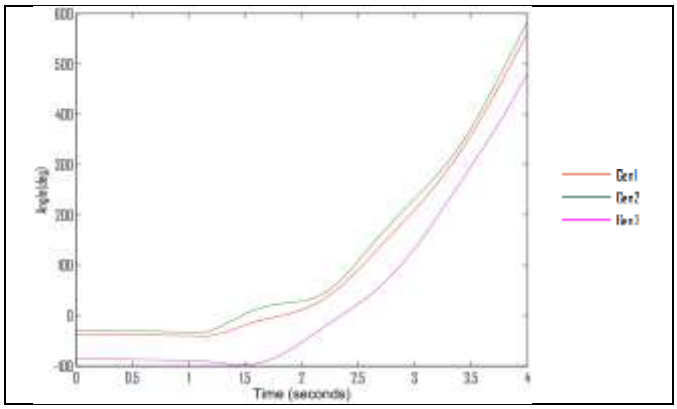

Fig IV.4c Absolute angle plot of all generators of IEEE 9 bus system

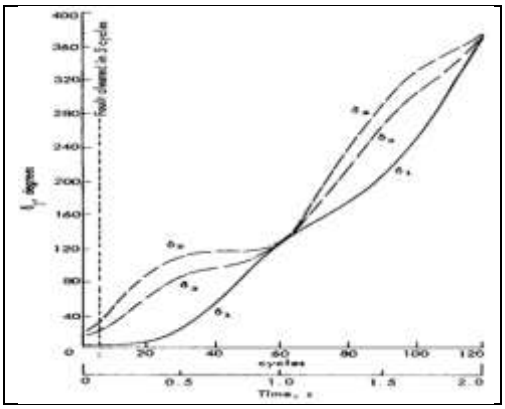

Fig IV.4d Classical example of Absolute angle all generators

IV.4.4. Case 3: Integration of the wind farm with IEEE 9-bus grid system.

In this study, a wind farm with a capacity of 51 MW and 280 MVA is connected to the standard IEEE 9-bus system. The wind farm is connected to the grid at bus 7 through bus 10. The wind farm consists of multiple 1.5 MW DFIG (Doubly-fed Induction Generator)

units, which are modelled as an equivalent machine representing the entire farm's output power. The connection between the wind farm (bus 10) and the grid (bus 7) is facilitated by a 230 kV transmission line and a step-up transformer (25/230 kV). Figure IV.5 illustrates the integration of the wind farm into an IEEE 9-bus system.

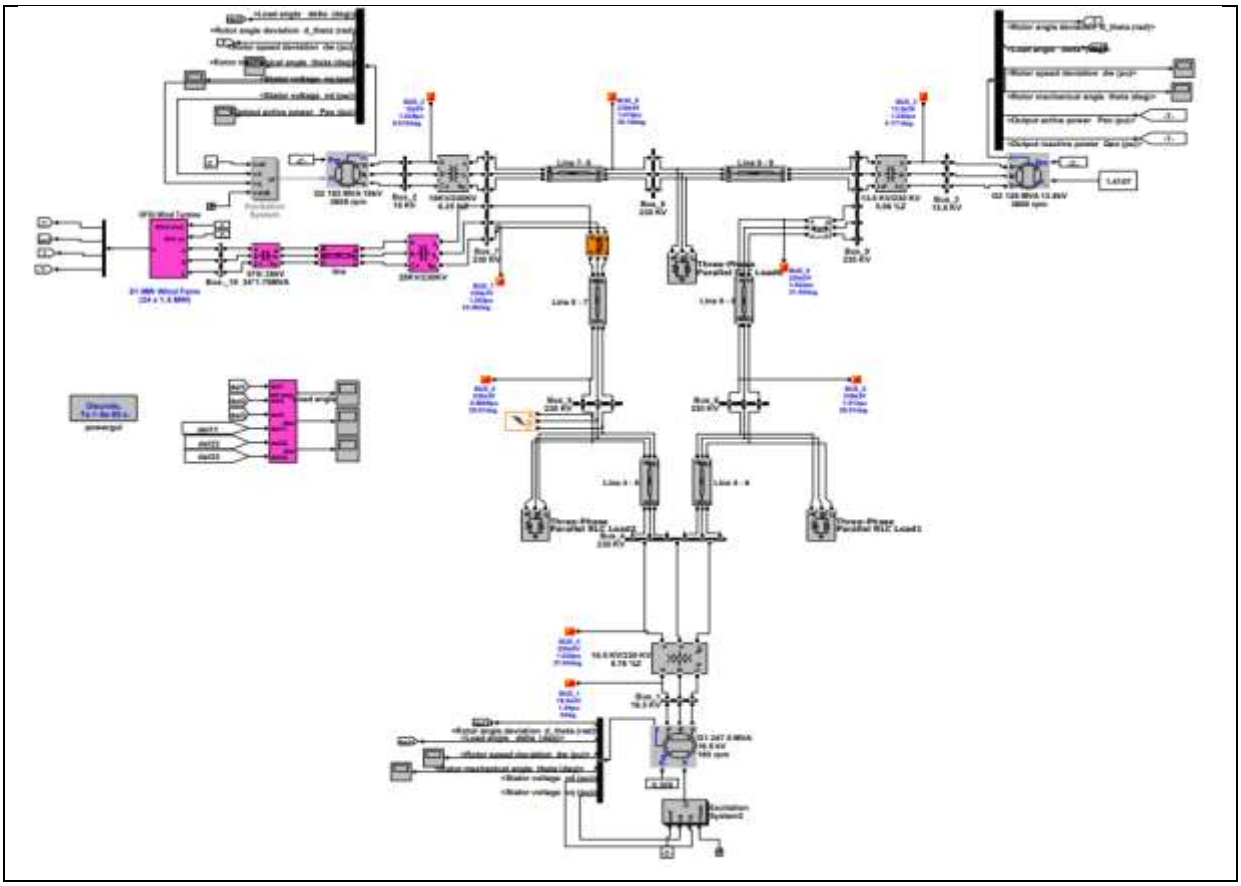

Fig IV.5 IEEE 9-Bus System integrated with a Wind farm

IV.4.4.1. Results and discussions

As previously mentioned, load flow analysis is crucial for both power system operation and dynamic simulation. The results of the load flow analysis of the remodelled model are presented in Table IV.2.

Table IV.2: Load flow analysis of remodelled model

Bus Number	Bus Name	PGen (MW)	PMax(MW)	PMin(MW)	QGen(Mvar)	QMax(Mvar)	QMin(MVar)
1	BUS1 16.5kV	23.8	250	10	38.68	300	-300
2	BUS2 18Kv	163	300	10	22.82	300	-300
3	BUS3 13.8Kv	85	270	10	-4.22	300	-300
10	WIND_FARM 13.8Kv	51	52	13.25	-16.76	16.76	-16.76

The dynamic analysis assesses the system's state after a three-phase fault or disturbance, focusing on the critical clearing time (CCT), which is the longest duration a disturbance can persist without affecting system stability. Identifying this time is crucial for ensuring stable operation during various disturbances. This study aimed to determine whether integrating a wind farm into the grid affects system stability and performance.

In this particular case study, a three-phase fault is applied to bus 5, which is a load bus, to analyse transient stability. The critical clearing time (CCT) was determined to be 0.75 seconds. The total simulation duration was 10 seconds, with the fault occurring at bus 5. The three-phase fault was cleared after 0.75 seconds, resulting in the disconnection of the line between bus 5 and bus 4. The simulation continued for an additional second before the tripped line was reconnected. Figure IV.6 illustrates the angles of two conventional generators, demonstrating system stability for a fault duration of 0.75 seconds. If the three-phase fault persists for longer than 0.75 seconds, the system becomes unstable.

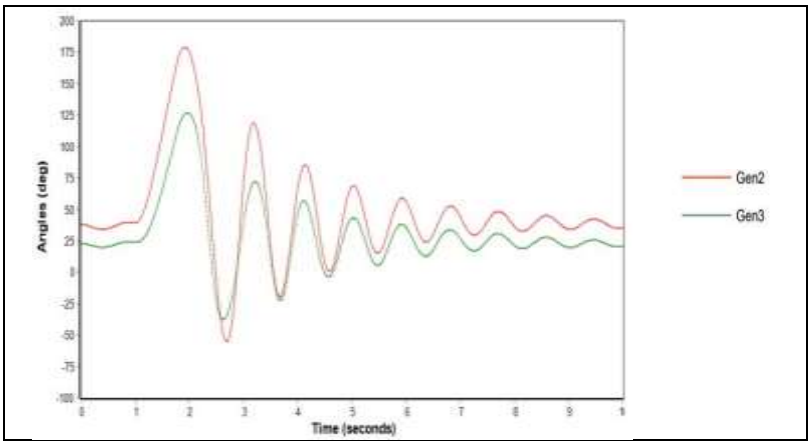

Fig IV.6 Angles of machines of bus 2 and bus 3

Figures IV.7a and IV.7b show the active power output of the wind farm and all the system's machines respectively. The figures clearly indicate that the wind farm's active power drops to nearly zero when the fault occurs. After the fault is cleared, the wind farm's active power quickly returns to its initial value of 0.3 pu, though some oscillations are present. These active power responses can be attributed to the rotor's acceleration, resulting in a larger negative slip during the fault. The observed oscillations may be due to the wind turbine model. Figure IV.7b illustrates the active power of all machines in the system, where a decrease in active power is noted post-fault, followed by significant oscillations in the conventional machines.

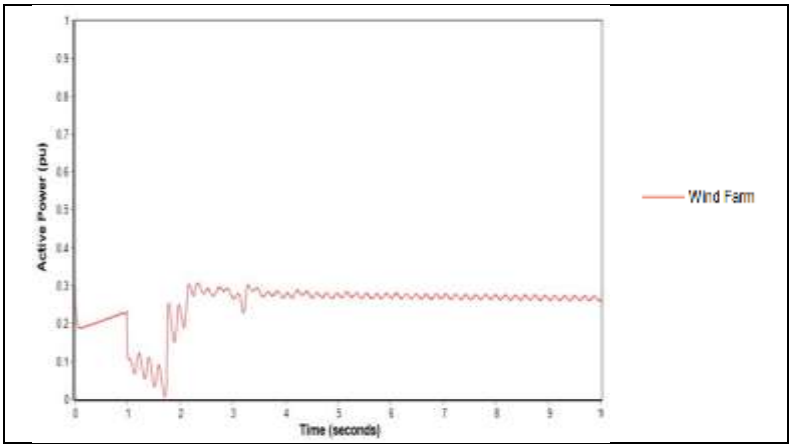

Fig IV.7a Active power of Wind Farm

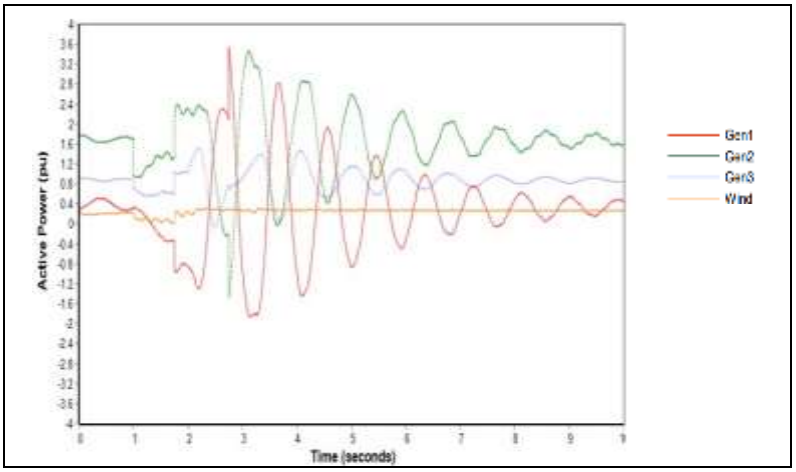

Fig IV.7b Active power of all machines

Figure IV.7c shows the reactive power outputs of the system's machines. Prior to the fault, the reactive power is stable at -0.168 pu (-16.8 MVAR). After the fault occurs, the wind farm's reactive power becomes unstable, oscillating between -0.400 pu and 0 pu. Significant fluctuations in reactive power are also observed in the conventional machines.

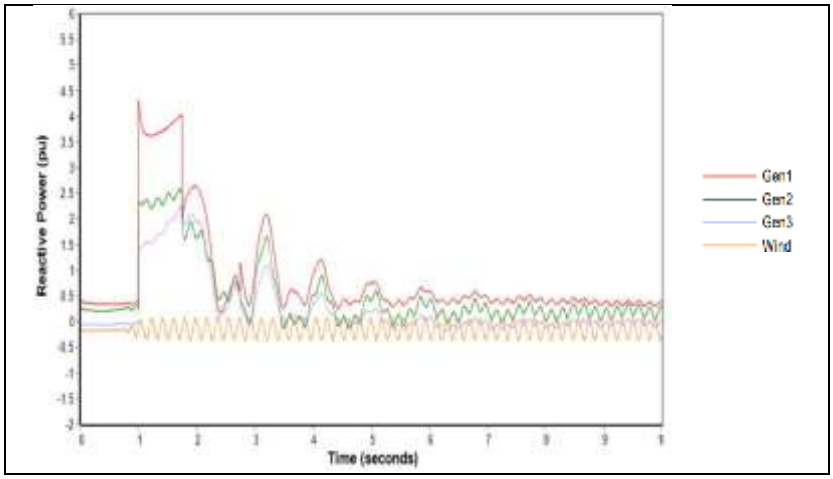

Fig IV.7c Reactive Power of all machines

Following the occurrence of the three-phase fault at bus 5, a voltage drop is observed across all machine buses. However, this drop is brief, and the voltages gradually return to their initial values. The voltage at the wind farm recovers to approximately 1 pu, with minor oscillations. Figure IV.8a illustrates the voltage behaviour of the entire system during the simulation, while Figure IV.8b specifically presents the voltage behaviour of the wind farm.

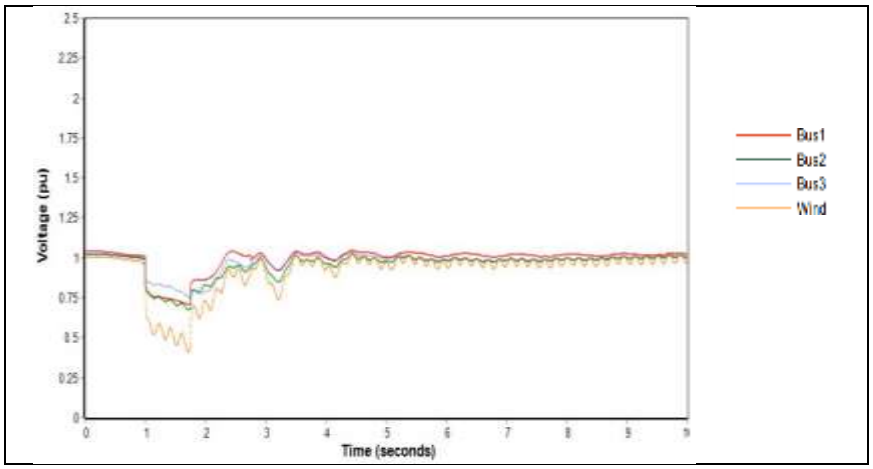

Fig IV.8a Voltage of all machines

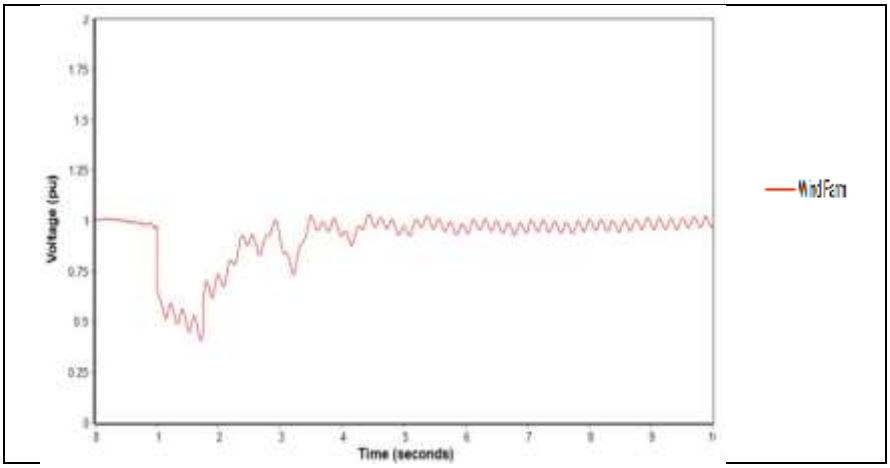

Fig IV.8b Voltage of all Wind Farm

As previously mentioned, the critical clearing time (CCT) identified for this study is 0.75 seconds. According to the simulation results, this duration should not be exceeded to maintain network stability. Exceeding this CCT leads to system instability. For instance, with a CCT of 0.8 seconds, the system becomes unstable after the fault. Figure IV.9a illustrates the active power for a CCT of 0.8 seconds, showing that the oscillations attempting to restore system stability are significantly wide. Similarly, the instability condition is observed in the reactive power of the network's machines, as shown in Figure IV.9b.

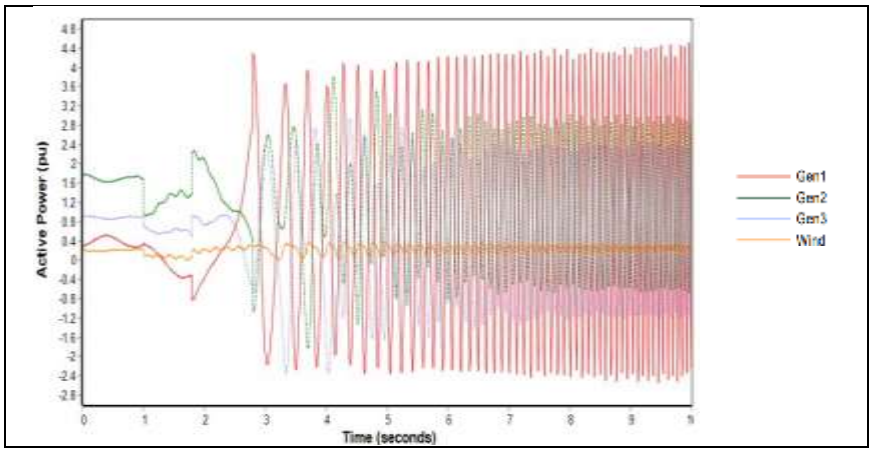

Fig IV.9a Active powers for CCT
0.8 sec.

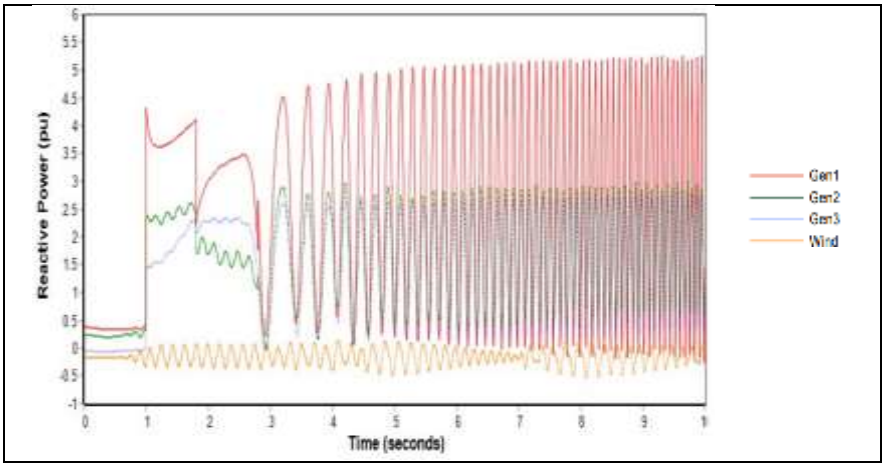

Fig IV.9b Active powers for CCT
0.8 sec.

Furthermore, the voltages remain unstable with significant oscillations following the fault. The voltages do not stabilize at their initial values, preventing the system from returning to its steady state condition. Figure IV.10 displays the voltages for a CCT of 0.8 seconds. Generally, the CCT should not exceed 0.75 seconds, as evidenced by the instability observed in the active and reactive power, as well as the voltage, in the figures provided.

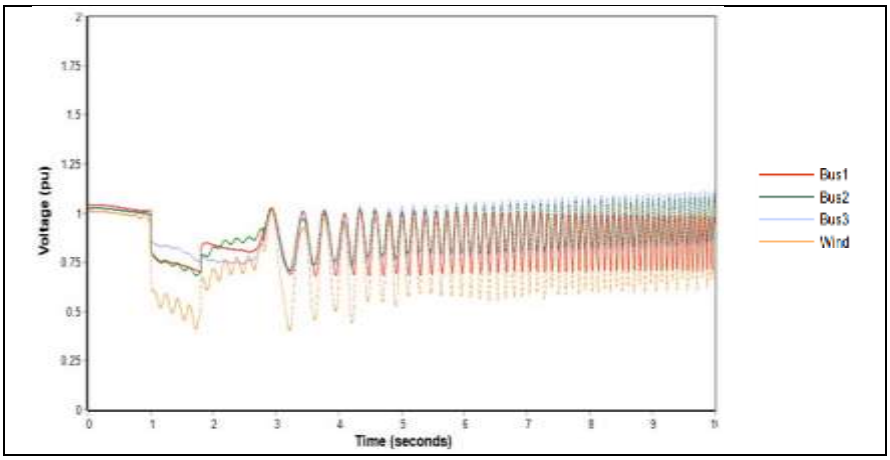

Fig IV.10 Voltages for CCT 0.8 sec

IV.4.5. Conclusion

This chapter comprehensively investigated the integration of a Doubly-Fed Induction Generator (DFIG) wind farm into the IEEE 9-bus system, examining both steady-state and dynamic (transient stability) aspects. The critical findings from this analysis include the determination of the Critical Clearing Time (CCT) for a three-phase fault at bus 5, which was found to be 0.75 seconds. Maintaining this duration is essential for grid stability

during disturbances, as exceeding this time can result in system instability. Furthermore, the integration of a 51 MW wind farm did not negatively impact the overall stability of the network. After a fault, the wind farm's active power, reactive power, and voltage outputs returned to their initial values, exhibiting only minor oscillations. Overall, the study demonstrates that integrating a DFIG wind farm into the IEEE 9-bus system is feasible without compromising grid stability, provided that the critical clearing time for faults is respected.

Additional considerations and future work for this study include the recognition that the wind farm model used was a simplified representation. Employing more complex models could provide deeper insights. The analysis focused on a single fault scenario, so further research involving different fault locations and types would offer a more comprehensive understanding. Future investigations could examine the impact of larger wind farms on the critical clearing time, explore advanced control strategies to enhance transient stability with wind farm integration, and analyse how different wind farm technologies affect overall grid performance.

GENERAL CONCLUSION

General Conclusion

The purpose of this study was to conduct a transient stability analysis of a power grid system integrated with a wind farm, using Critical Clearing Time (CCT) to derive conclusions through MATLAB/Simulink simulations. The study began with an overview of renewable energy and the growth of wind power generation, ending with an outline of the entire thesis.

The second part looked into the basics of wind turbine technology, including the types of turbines and their components. It also explored the principles of wind power conversion and the various generators used in wind energy generation.

The third section focused on the concept and theories of transient stability analysis in power generation, highlighting its importance and challenges. It also offered an overview of techniques and methods used in transient stability analysis, with detailed models of the Doubly-Fed Induction Generator (DFIG) and the IEEE 9-Bus system.

In the final chapter, a detailed simulation and discussion was carried out. This section included simulations of the wind farm independently, the IEEE 9-Bus system alone, and the integration of the two systems. The results demonstrated that the wind farm could withstand fluctuations in wind speed, consistently reaching its steady state. When integrating the two systems, the following conclusions were drawn:

- The critical clearing time (CCT) for an existing grid system was determined to be 0.36 seconds, within which the system always regained stability.
- The critical clearing time (CCT) for an integrated system was determined to be 0.75 seconds, within which the system always regained stability.
- Exceeding the CCT led to the instability of the entire system.

The study concluded that integrating a wind farm into an IEEE 9-Bus system does not negatively impact the stability of the system. It increased the CCT hence increasing the stability of the system. The grid consistently achieved its steady state, and all transients were effectively eliminated. This research demonstrates the feasibility and stability of integrating wind energy into traditional grid systems, contributing valuable insights for future renewable energy projects.

References

1. Intergovernmental Panel on Climate Change (IPCC). "Global Warming of 1.5°C". https://www.ipcc.ch/site/assets/uploads/2019/08/. 2018
2. International Energy Agency (IEA). "Renewables 2021 Analysis and Forecast to 2026." http://www.oecd.org/about/. 2021.
3. Global Wind Energy Council (GWEC). (2020). "Global Wind Report 2020."
4. "Wind Energy Explained: Theory, Design and Application" by James F. Manwell, Jon G. McGowan, and Anthony L. Rogers (John Wiley & Sons, 2009).
5. World Wind Energy Association (WWEA). (2022). "World Wind Energy Report 2022."
6. Tómasson, E. "Impact of High Levels of Variable Renewable Energy on Power System Generation Adequacy: Methods for analyzing and ensuring the generation adequacy of modern, multi-area power systems" (Doctoral thesis). Stockholm, Sweden: KTH Royal Institute of Technology, 2020.
7. Pai, M. A. "Energy Function Analysis for Power System Stability." CRC Press, 2018.
8. Amilarasi, T., & Elango, M. K. "Analysis of Impact on Rotor Angle Stability of DFIG Wind Turbines Employing STATCOM," 2016.
9. Kundur, P. "Power System Stability and Control." McGraw-Hill, 1994.
10. Archer, C. L., & Jacobson, M. Z. "Evaluation of Global Wind Power." Journal of Geophysical Research: Atmospheres, 110(D12), 2005.
11. Ackermann, T., & Soder, L. "Wind Power in Power Systems." 2005.
12. Manwell, J. F., McGowan, J. G., & Rogers, A. L. "Wind Energy Explained: Theory, Design and Application." John Wiley & Sons, 2009.
13. Cai, Q., Chen, D., Yang, N., & Li, W. "A Novel Semi-Spar Floating Wind Turbine Platform Applied for Intermediate Water Depth." Sustainability, 16, 1663. https://doi.org/10.3390/su16041663. 2024.
14. Schaffarczyk, A,. "Understanding Wind Power Technology: Theory, Deployment and Optimisation." (G. Roth, Trans.). John Wiley & Sons, Ltd. 2014.
15. Jiang, Y., Chen, P., Wang, S., Cheng, Z., & Xiao, L. "Dynamic responses of a 5 MW semi-submersible floating vertical-axis wind turbine: A model test study in the wave basin." Ocean Engineering, 296, 117000. 2024.
16. Hansen, M. H,. ''Wind Energy : Fundamentals, Resource Analysis and Economics.''Springer. 2015.
17. B. Beltran., ''Contribution à la Commande Robuste des Eoliennes à Base de Génératrices Asynchrones Double Alimentation : Du Mode Glissant Classique au Mode Glissant d'Ordre Supérieur.'' , PhD Thesis (in French), University of Brest, 2009.
18. Musgrove, P. J,. "Wind Energy Conversion Systems." CRC Press. 2014.
19. Kabat, S.R., Panigrahi, C.K., Ganthia, B.P., Barik, S.K., Nayak, B. "Implementation and Analysis of Mathematical Modeled Drive Train System in Type III Wind Turbines Using Computational Fluid Dynamics." Advances in Science and Technology Research Journal. 2022.
20. Perdana, A. ''Dynamic Models of Wind Turbines: A Contribution towards the Establishment of Standardized Models of Wind Turbines for Power System

Stability Studies.'' Ph.D. dissertation, Chalmers University of Technology, Gothenburg, Sweden. 2008.
21. O. A. Lara, N. Jenkins, J. Ekanayake, P. Cartwright, M. Hughes, ''Wind Energy Generation: Modelling and Control.'' Chichester, UK: Wiley, 2009.
22. A. W. Manyonge, R. M. Ochieng, F. N. Onyango , J. M. Shichikha, "Mathematical Modelling of Wind Turbine in a Wind Energy Conversion System: Power Coefficient Analysis", Applied Mathematical Sciences, Vol. 6, no. 91, pp. 4527 – 4536, Apr. 2012.
23. Dongare, U. V., Umre, B. S., & Ballal, M. S.''Rotor winding inter-turn short-circuit fault detection in wound rotor induction motors using Wing Technique''. Journal of Electrical Engineering, 22, 614–628. 2022.
24. Tsantzalis, S. ''Transient stability analysis of a power system with the integration of wind energy (Master's thesis). University of Thessaly, School of Engineering, Department of Electrical and Computer Engineering. Supervisor, 2021.
25. P. Kundur, J. Paserba, V. Ajjarapu, G. Andersson, A. Bose, C. Canizares, N. Hatziargyriou, D. Hill, A. Stankovic, C. Taylor, T. Van Cutsem, and V. Vittal, "Definition and classification of power system stability IEEE/CIGRE joint task force on stability terms and definitions," IEEE Trans. Power Syst., vol. 19, 2004.
26. Goncharovskiy, O. V., Yuzhakov, A. A., Storozhev, S. A., &Nikulin, V. S. ''A Starter–Generator Based on a Synchronous Machine with Permanent Magnets.'' Journal of Electrical Engineering, 94, 820–824. 2023.
27. Ilahi Bakhsha, F., Shees, M. M., &Asghar, M. S. J. ''Performance of Wound Rotor Induction Generators with the Combination of Input Voltage and Slip Power Control.'' Alternate Hydro Energy Centre Indian Institute of Technology RoorkeeRoorkee, India. Singhania University, Rajasthan, India. Department of Electrical Engineering Aligarh Muslim University Aligarh, India. 2013.
28. Metatla, S., Mekhtoub, S., Nesba, A., Colak, I., &Ouadah, M. ''Analytical design of fractional order proportional-integral controller for enhanced power control of doubly-fed induction generator.'' Rev. Roum. Sci. Techn.–Électrotechn. etÉnerg., 65(1-2), 109–115. 2020.
29. Ebeed, M. ''Enhancement Protection and Operation of the Doubly-fed Induction Generators during Grid Fault'' (M.Sc. Thesis). Faculty of Engineering, South Valley University, Qena, Egypt. 2013.
30. Sun, T. ''Power Quality of Grid-Connected Wind Turbines with DFIG and Their Interaction with the Grid'' (Ph.D. thesis). Faculty of Engineering & Science, Aalborg University, Denmark. 2004.
31. P,. Radhakrishnan., J. ''Transient stability analysis of grid with DFIG wind power plant'' (Master's thesis). California State University, Northridge. 2014.
32. Pai, M. A. ''Energy Function Analysis for Power System Stability.'' Springer Science & Business Media. 2012.
33. Toft, A. K. ''Direct methods for transient stability analysis and contingency screening in power systems.'' (Master's thesis, FMH606, Electrical Power Engineering). University of South-Eastern Norway. 2023.
34. A. Abo-Khalil, "Synchronization of DFIG Output Voltage to Utility Grid in Wind Power System", Science Direct, Elsevier, Renewable Energy, Vol. 44, Iss. 1, PP.

193/198, 2012.
35. Hadi, S. A., &Dahal, K. P. ‘’Transient Stability of Power Systems: Theory and Practice.’’ CRC Press. 2021.
36. Gasch, R., &Twele, J. "Wind Power Plants: Theory and Design." Springer. 2018.
37. Zhou, L., Roy, S. B., &Xia, G. ‘’Weather, Climatic and Ecological Impacts of Onshore Wind Farms.’’ Department of Atmospheric and Environmental Sciences, University of Albany. 2022.
38. D. Zouheyr., L. Baghli., T. Lubin., B,. Abdelmadjid. ‘’Grid Side Inverter Control for a Grid Connected Synchronous Generator Based Wind Turbine Experimental Emulator.’’ European Journal of Electrical Engineering, 2021.
39. Kamarzarrin, M., Refan, M.H. ‘’Intelligent Sliding Mode Adaptive Controller Design for Wind Turbine Pitch Control System Using PSO-SVM in Presence of Disturbance.’’ J Control AutomElectrSyst 31, 912–925 (2020). https://doi.org/10.1007/s40313-020-00584-x
40. Palepogu, K. R., & Mahapatr, S. ‘’Synchronous Pitch and Yaw Orientation Control of a Twin Rotor MIMO System Using State Varying Gain Sliding Mode Control.’’ Electrical Engineering Research Article. 2024.
41. Weng, C. Y. ‘’Transient Stability Analysis of Power Systems with Energy Storage.’’ Master's thesis, Case Western Reserve University. 2013.
42. Pertl, M., Weckesser, T., Rezkalla, M., &Marinelli, M. ‘’Transient stability improvement: a review and comparison of conventional and renewable-based techniques for preventive and emergency control.’’ 2017.
43. Cacciolatto, A. ‘’Wind Farm Sliding Mode Control and Energy Optimization with Fatigue Constraints’’ (Master's thesis, Politecnico di Torino). 2019.
44. Kabat, S.R., Panigrahi, C.K., Ganthia, B.P., Barik, S.K., Nayak, B. "Implementation and Analysis of Mathematical Modeled Drive Train System in Type III Wind Turbines Using Computational Fluid Dynamics." Advances in Science and Technology Research Journal. 2022.
45. Glover, J. D., &Sarma, M. S. "Power System Analysis and Design." Cengage Learning. 2011.
46. B, Shonhiwa. ‘’Impact of the integration of Distributed Generation on Power System Voltage Stability’’ (Master's thesis). University A.MIRA-BEJAIA, People's Democratic Republic of Algeria. 2023.
47. Anand, A. K., & Rathor, G. P. ‘’Load Analysis of Statcom with Voltage Regulation Controller Based Standalone Wind Energy System.’’ IJO-SCIENCE, 5(7). https://doi.org/10.24113/ijoscience.v5i7.215. 2019.